Superficial High Dose Rate Brachytherapy for the Treatment of Lower Eyelid Carcinomas

Holly Stephens

Thesis submitted for the degree of

Master of Philosophy (Sciences)

In the School of Physical Sciences
The University of Adelaide

Supervisors:
Dr Judith Pollard
Dr Alexandre Santos
A/Prof Tanya Kairn

March 2021

Contents

Abstract

Basal and Squamous cell carcinomas of the eyelid account for a large proportion of skin cancers. Historically the eyelid has been a challenging area to successfully treat and achieve good cosmetic outcomes for patients. This work aims to establish a new way to treat lower eyelid basal and squamous cell carcinomas by using an intraluminal catheter and a high dose rate iridium brachytherapy source.

Different mould techniques were used to place the catheter under the lower eyelid, with the aid of a stereotactic head phantom. The optimal mould was then scanned, and a treatment plan was established using Oncentra Brachytherapy software, in combination with the AAPM TG43 algorithm for dose.

Two methods were used to verify this plan. Gafchromic film was placed under the mould and analysed using FilmQA Pro software. For organs at risk, optically stimulated luminescence dosimeters were used for point doses and read out using microstarii software.

Different setups involving varying levels of bolus around the catheter were tested to eliminate the air gaps to remove the uncertainty of density differences.

The results showed that an effective treatment plan can be created using an intraluminal catheter and 6 mm of bolus between the skin and catheter to produce an appropriate dose distribution in the patient for the GEC-ESTRO recommended fractionation scheme of 4 Gy per fraction, with a total of 10–12 fractions, 3 times a week for a total dose 40–48 Gy.

Declaration

I certify that this work contains no material which has been accepted for the award of any other degree or diploma in my name in any university or other tertiary institution and, to the best of my knowledge and belief, contains no material previously published or written by another person, except where due reference has been made in the text. In addition, I certify that no part of this work will, in the future, be used in a submission in my name for any other degree or diploma in any university or other tertiary institution without the prior approval of the University of Adelaide and where applicable, any partner institution responsible for the joint award of this degree.

I give permission for the digital version of my thesis to be made available on the web, via the University's digital research repository, the Library Search and through web search engines, unless permission has been granted by the University to restrict access for a period of time.

I acknowledge the support I have received for my research through the provision of an Australian Government Research Training Program Scholarship.

Holly Stephens

18/08/2019

Acknowledgements

I would first like to thank my thesis supervisors, Judith Pollard, Alexandre Santos and Tanya Kairn. They were available for advice whenever I ran into a trouble spot or had a question about my research or writing. They consistently allowed me to conduct my own work, but steered me in the right the direction whenever they thought I needed it, or became side tracked.

I would also like to thank the local radiation therapists and radiation oncologists who were involved in the validation of clinical protocols for this research project, especially Candice Deans and David Schlect without their passionate participation and input, the validation and clinical work could not have been successfully conducted.

I must express my very profound gratitude to my parents and to my husband for providing me with unfailing support and continuous encouragement throughout my years of study and through the process of researching and writing this thesis. This accomplishment would not have been possible without them. Finally, thanks must go to the never ending support of my two dogs Skadi and Bernie for always listening to me read my thesis aloud for clarity, and to my cat Meg for always sitting on my keyboard at the most inappropriate times, but always doing so with an evil grin. Thank you.

List of Tables

List of Figures

Abbreviations

AAPM	American Association of Physicists in Medicine
ACDS	Australian Clinical Dosimetry Service
ACROP	Advisory Committee on Radiation Oncology Practice
BCC	Basal Cell Carcinoma
CT	Computed Tomography
Cu	Copper
CV	Coefficient of Variation
DICOM	Digital Imaging and Communications in Medicine
d_{max}	Depth of Maximum Dose
EBT3	External Beam Therapy Three
ECF	Element Correction Factor
ESTRO	European SocieTy for Radiotherapy and Oncology
GEC	Groupe Européen de Curiethérapie
Gy	Gray
HDR	High Dose Rate
IAEA	International Atomic Energy Agency
ICRP	International Commission on Radiological Protection
IMRT	Intensity-modulated radiation therapy
Ir-192	Iridium 192
IVD	In Vivo Dosimetry
kV	Kilovoltage
LiF	Lithium Fluoride
MOSFET	Metal Oxide Semiconductor Field Effect Transistor
MRI	Magnetic Resonance Imaging
MU	Monitor Unit

MV	Megavoltage
OAR	Organ At Risk
OSLD	Optically Stimulated Luminescence Dosimeter
PDD	Percentage Depth Dose
PMT	Photomultiplier Tube
PTV	Planning Target Volume
QA	Quality Assurance
QC	Quality Control
QR	Quick Response
SCC	Squamous Cell Carcinoma
STEEV	Stereotactic End-to-End Verification
TG	Task Group
TLD	Thermoluminescent Dosimeter
TPS	Treatment Planning System
VMAT	Volumetric Modulated Arc Therapy
WHO	World Health Organization

1. Introduction

Basal cell carcinoma (BCC) and squamous cell carcinoma (SCC) account for 90% of all eyelid malignancies, and 5-10% of skin cancer cases, 50% occurring in the lower eye region (Manghani and Khan, 2016). Surgery has long been the preferred method of treating BCC and SCC on other parts of the skin, however this presents a problem for eyelids due to the poor cosmetic outcomes, low levels of underlying tissue and longer recovery periods (Guix et al., 2000b) Early radiation treatment techniques (from the 1950s) included the use of kV radiotherapy, cobalt-60 machines (Frakulli et al., 2015) and interstitial brachytherapy using Ir-192 wires (Daly et al., 1984)

Early High Dose Rate (HDR) interstitial treatments of eyelid carcinomas using implanted Ir-192 wires produced 'definitive cure' rates of up to 97.4% (Daly et al., 1984) However, radiation safety concerns (Arnott et al., 1985) and technological developments have led to widespread abandonment of the use of Ir-192 wires. Today, HDR brachytherapy treatments are delivered using remote Afterloaders, with small, reusable high activity Ir-192 sources attached to drive trains.

In 2007 the first published paper on Afterloader based HDR brachytherapy specific to eyelids appeared (Martinez-Monge and Gomez-Iturriaga, 2007). The paper provided a case study where a single patient was treated using interstitial brachytherapy following surgical excision of the tumour. The HDR brachytherapy catheter was embedded in the patient's remaining eyelid tissue for treatment delivery. It was noted that the larger size of the catheter needed to deliver the Afterloaders HDR source was an issue for treatment. The report noted a good outcome for the patient, both cosmetically and in terms of tumour control.

Interstitial HDR treatments using implanted needles and catheters have subsequently been shown to produce positive outcomes with good cosmesis (Krengli et al., 2014), (Azad and Choudhary, 2011). The broad adoption of these techniques has, however, been limited by the need for needle or catheter implantation under local anaesthetic, and the resulting sterilization and surgical demands, patient discomfort and clinical limitations on the number of treatment fractions that can reasonably be delivered to each patient.

This study aimed to develop a technique using HDR brachytherapy to treat lower eyelid carcinomas, using superficial catheters as surface applicators. Film dosimetry, optically stimulated luminescence dosimetry and head phantoms were used to come up with an optimal treatment technique, to overcome anatomical difficulties and deliver non-surgical treatments.

Chapter two reviews the literature of current treatments for basal and squamous cell carcinomas, treatment planning limitations and algorithms, superficial carcinoma treatments and dose measurement techniques for brachytherapy. The thesis then provides a description of the implemented method using a single superficial catheter and custom surface moulds with a HDR Ir-192 source and associated dosimetry (chapter three), as well as dosimetry analysis of film measurements (chapter four), optically stimulated luminescence dosimeters (chapter five) and conclusions (chapter six). Clinical protocols and treatment instructions are listed in the appendices.

2. Literature Review

2.1 Carcinomas and other lesions of the skin and eyelid

Anatomically, the orbit is conical, and is defined by bony margins, approximately 6 mm thick (Turvey and Golden, 2012, Xu et al., 2017). Contents of the orbit include the eye, optic nerve and muscles (Snell and Lemp, 2013). Eye movement is controlled by the IIIrd, IVth and VIth nerves (Symonds et al., 2012). The inner surface of the eyelids is lined with a membrane called the conjunctiva, covering anterior to the eye, to the corneoscleral junction. The lacrimal glands (these glands secrete tears) reside on the lower eyelid, complimented with a few located on the upper lateral part of the orbit (Sullivan et al., 2003). The tears are drained to the nose via the nasolacrimal duct (Paulsen, 2012).

Both benign and malignant tumours can occur at the orbit. Malignant disease can be further differentiated into primary or secondary / metastatic disease (Frederick L et al., 2013).

The two most common primary tumours of the orbit region are basal cell carcinoma (BCC) and squamous cell carcinoma (SCC), both occurring on the face, especially around the lower eyelid (Ouhib et al., 2015). Other primary tumours are: lacrimal gland, nasolacrimal duct (both skin based) and lymphoma, melanoma, rhabdomyosarcoma, optic nerve glioma and retinoblastoma (orbital and intraocular) (Symonds et al., 2012).

Basal Cell carcinomas are the most common type of eyelid tumours, accounting for 90% of cases (Frakulli et al., 2015). The average age at diagnosis is 68 years, and the ratio of cases in men to women is 4:1 (Weinstock et al., 1991). Basal cell carcinomas are found around the face, they are poorly demarcated and often ulcerated in appearance (Crowson, 2006). They spread quite slowly, less than 0.1% metastasise through the lymphatic system to secondary sites of the liver, lung and bones (Ozgediz et al., 2008, Safai and Good, 1977).

Squamous Cell Carcinomas are less common (approximately 9%), however have the same average age at diagnosis and sex ratios as basal cell carcinomas (Reifler and Hornblass, 1986). A squamous cell carcinoma is pearlier in appearance, and is much more likely to metastasise (up to 40%) and to include perineural invasions (Firnhaber, 2012, Soysal and Markoç, 2007). The locations of secondary tumours are lung, liver and bone (Kotwall et al., 1987).

For diagnosis, a history and physical exam are completed. The physician also palpates for the extent of the non-superficial lesion, and performs a cranial nerve and lymph node examination. Definitive diagnosis is obtained by performing a biopsy, along with a CT scan and MRI (if lymph node involvement is suspected). A CT scan is especially important if there is any indication that there is a possibility of bone invasion.

2.2 Existing Skin Carcinoma Treatment Techniques

The six major treatment techniques for basal and squamous cell carcinomas are cryotherapy, electrodessication, chemotherapy, surgery, Mohs microsurgery and radiation therapy. All six techniques are recommended treatments, depending on the tumour type and location (Hansen and Roach, 2006). Cryotherapy, curettage and electrodessication techniques are all recommended for small, superficial tumours with clearly defined margins. Curettage and electrodessication techniques are inadvisable when treating recurrences or cancers presenting over scar tissue, cartilage or bone (Hansen and Roach, 2006). Chemotherapy is generally applied topically and only if the cancer is confined to the epidermis. Chemotherapy is not normally used systemically however when used it has a partial response of 60-70% and a complete response of 30% (Hansen and Roach, 2006).

There are two surgery options – conventional surgery and Mohs micrographic surgery. Traditional surgery has reconstructive advantages. Mohs micrographic surgery gives maximum skin sparing and concomitant pathologic examination of

each horizontal and deep margin. If perineural invasion is present, radiation therapy follow-up post op is recommended. Follow-up radiation is also recommended if there are positive margins, the primary tumour is greater than 3 cm, there is extensive skeletal muscle invasion, bone or cartilage invasion or if the primary is a squamous cell carcinoma of the parotid (Hansen and Roach, 2006).

If there are positive margins present after surgical excision, recurrence rates depend on the type of tumour. For basal cell carcinomas, one third recur if the lateral margin is positive; recurrence is greater than 50% if the deep margin is positive. Most squamous cell carcinomas with a positive margin can recur loco regionally with a less than 50% salvage rate if there is positive local node involvement. Additional treatment is recommended if there is a positive margin, and this is to be done immediately if treating a squamous cell carcinoma (Hansen and Roach, 2006).

Contraindications to radiation therapy include patients younger than 50 years due to poor cosmesis, post radiation recurrences (in this instance the recommendation is to use Mohs microsurgery), areas that are prone to trauma (hand, belt line), poor blood supply, high occupational sun exposure, an impaired lymphatic system or exposed bone or cartilage (Hansen and Roach, 2006).

For BCC and SCC of the eyelids, local excision has been the usual form of treatment if the tumour is 5 mm or less, along with radiotherapy (either superficial or electrons). A margin of 5 mm is used for BCC, and 10 mm is generally acceptable for SCC, due to their ability to metastasise easily (Kaprealian et al., 2010).

External beam radiation therapy is effective if the lesion is between 5 and 20 mm, however a lead shield should be used to protect the lens, after ophthalmic

anaesthetic drops have been used. When using an eyeshield mild conjunctivitis can occur but the rate of cataracts becomes negligible (Frakulli et al., 2015). Recommended fractionation for a 5 to 20 mm tumour is 48 Gy in 16 fractions using 100 keV and 0.19 mm Cu equivalent (Kaprealian et al., 2010).

2.3 Skin Carcinoma Treatments Using External Beam Radiation Therapy

Superficial external beam radiation therapy modalities are widely used to treat skin lesions. Orthovoltage techniques need less of a margin on the skin surface, are cheaper to perform than high energy electron therapy, the maximum dose delivered is at the skin surface and the beam can be collimated with a lead cut-out. The thickness of the lead needs to be at least 0.95 mm for energies less than 150 keV and greater than 1.9 mm for energies greater than 150 keV. The prescription isodose of 90% needs to encompass the tumour. Orthovoltage techniques are not used if the tumour is greater than one-centimetre-deep, or if bone is involved. In these cases, high energy megavoltage (MV) radiotherapy should be used to give better dose coverage. The relative biological effectiveness of photon beams from orthovoltage techniques is 10-15% higher than the relative biological effectiveness of megavoltage photon and electron beams, hence the daily prescription should be modified to take this into account.

Around the ocular region, the lens, cornea, nasal septum and teeth (for extreme cases) should be shielded from primary radiation. Thin strips of wax over the eyelid can help with conjunctivitis stemming from the use of a lead eye shield. (Hansen and Roach, 2006)

Margins applied to the treatment fields are dependent on the size of the primary tumour. For tumours less than 2 cm in the largest dimension, a 0.5 to 1 cm margin is sufficient, whereas if it is larger than 2 cm then a margin of 1.5 to 2 cm should be used. The deep margin is 0.5 cm past the actual depth of the tumour, regardless of size.

Common complications that can arise from external beam radiation treatment can include telangiectasias, skin atrophy, hypopigmentation, skin necrosis (occurring in approximately 3% of cases), osteoradionecrosis (occurring in approximately 1% of cases), chondritis/cartilage necrosis (this becomes rare if the fractionation regime is less than 300 cGy per day), hair loss and loss of sweat gland function (Guix et al., 2000a, Frakulli et al., 2015).

General follow-up depends on the type of tumour. For basal cell carcinomas, a follow-up physical examination every 6-12 months for life, and for squamous cell carcinomas 3-6 months for the first two years, then 6-12 months for the following 3 years, then annually for life. This changes to 3 monthly for 2 years, 4 monthly for the following 2 years, 6 monthly for the next 2 years and annually after that for squamous cell carcinomas with regional involvement.

2.4 Skin Carcinoma Treatments Using HDR Brachytherapy

Early HDR brachytherapy treatments of the skin used Ir-192 wires, which needed to be manually cut and inserted into the patient's tissue (Daly et al., 1984). This use of Ir-192 wires has been largely abandoned in developed countries due to radiation safety concerns around the preparation and use of Ir-192 wires (Arnott et al., 1985) combined with the increasing availability of remote After-loading units and associated computerised treatment planning systems.

Sophisticated remote After-loading systems permit the use of purpose-designed applicators for superficial HDR brachytherapy treatments. For example the Leipzig (Niu et al., 2004) and Valencia (Tormo et al., 2014, Delishaj et al., 2015) applicators both position the source at the top of a shielded, conical air volume, and deliver the treatment via a circular end plate (usually 20 mm or more in diameter)

Two things make this type of applicator unsuitable for use in eyelid treatments, the first being the need for the end plate to make uniform contact with the patient's skin to achieve accurate dose delivery, which is unachievable for irregular skin surfaces and the second being the steep dose fall off provided by the applicators (e.g. 10% per mm) which makes them unsuitable for treating at depths greater than 5 mm (Tormo et al., 2014). Custom surface moulds can overcome the irregular shape to provide best contact with minimal gaps.

For eyelid, implanted catheters for Afterloader sources (Azad and Choudhary, 2011) have replaced the use of implanted Ir-192 wires (Daly et al., 1984) However, there are issues with catheter diameter (Martinez-Monge and Gomez-Iturriaga, 2007) and the need for surgical implantation.

2.5 HDR Brachytherapy Treatment Planning

There are several different commercial remote After-loading systems that can be used to deliver HDR brachytherapy treatments with an Ir-192 source.

The source configuration varies with vendor, however most systems use a single capsule, less than 5 mm long and less than 1 mm in diameter, containing one or more Ir-192 rods or pellets (Rivard et al., 2004) which is attached to the end of a drive wire.

During a HDR brachytherapy treatment, the source is driven to one or more pre-programmed 'dwell positions' within applicators or catheters that may be placed on the patient's skin or implanted in the patient's tissue. Remote Afterloader based HDR brachytherapy treatment planning is therefore a process of specifying the dwell positions and dwell times that will combine to make up the treatment dose.

Ir-192 has a half-life of 73.8 days, and decays via beta and electron capture. The decay of one Ir-192 nucleus gives rise to an average of 2.4 photons which can each have one of 44 possible photon energies ranging from 7.8 to 1378 keV. One iridium decay also gives rise to 0.95 beta decay electrons which are emitted in a continuous spectrum between 0 and 669 keV.

Atomic electrons can also be emitted in this process with varying discreet energies between 11 and 1378 keV. This gives rise to the average total photon output of one Ir-192 event of 813 keV, giving $\frac{813}{2.4} = 340$ keV per photon, and an average energy of 216 keV per electron.

In dose calculations it is conventional to ignore the electron component, which is largely absorbed by the stainless steel source encapsulation, and does not contribute clinically to a significant dose to the patient.

Generally speaking, the process of HDR treatment planning usually consists of the following steps (Ouhib et al., 2015):

1. The planning treatment volume (PTV) and organs at risk (OARs) or reference points are defined
2. The treatment applicator or implant geometry is defined
3. The dwell positions within the applicator or implant are defined and optimal dwell times are calculated (either manually or by using inverse planning algorithms)
4. The treatment plan is evaluated and refined, doses to targets and OARs checked, hot and cold spots are mitigated and the plan is approved for treatment.

The computerised treatment planning system calculates and recalculates dose as needed throughout steps three and four.

Relevant dose metrics are recorded in patient files and the plan is sent for checking and delivery.

When a skin treatment is planned for delivery, using a Leipzig or Valencia applicator, step two consists of selecting the applicator from a list of pre-defined geometries, based on the applicator diameter that is needed to cover the target, and at step three a single dwell position is defined, with a dwell time calculated to deliver the prescribed dose at the depth of the target (Ouhib et al., 2015).

When an interstitial (implanted) catheter is used to treat a skin carcinoma, the catheter geometry can be defined by locating the implant in 2D radiographic or 3D computed tomographic geometry in the treatment planning system (Azad and Choudhary, 2011). Dwell positions are then specified along a line defined by the catheter or virtual geometry, with dwell times calculated to achieve a prescribed dose at a particular distance from the source (Azad and Choudhary, 2011). Due to the substantial disadvantages of using conventional superficial applicators and interstitial catheters for eyelid treatments, as discussed in section 2.4, this study developed an alternative method, based on the use of superficial catheters and patient specific custom moulds.

“Custom moulds are designed to follow the contour of the skin surface and precisely house the catheters at a specific distance” (Ouhib et al., 2015). Custom moulds have been successfully used during HDR brachytherapy treatments of the ear (Alam et al., 2011), hand (Somanchi et al., 2008) and scalp (Semrau et al., 2008) and are therefore a promising option for treating the eyelid.

Treatment planning for skin treatments with custom moulds involves: defining a target, choosing a catheter, creating a mould around the catheter and CT imaging patient with the mould in situ. The steps one to four above, are then followed as usual.

Care needs to be taken when treating cancers of this area with radiotherapy. Cataracts can occur when the lens dose is as little as 2 Gy, however in patients over 70 they can occur due to other factors, such as diabetes, steroids and other medications (Hansen and Roach, 2006).

Radiation cataracts can be distinguished by their location – the damaged cells are located anterior central to the lens; the cataract is formed at the central rear of the eye. Cataracts usually appear 2-3 years after radiotherapy. They can generally be surgically removed in the standard way. Other areas include the sclera, which can tolerate doses up to 100 Gy, and the retina, cornea and lacrimal apparatus which can tolerate up to 50 Gy, however it is suggested to limit the dose to the lacrimal apparatus to below 30 Gy if possible to help prevent reduced tear production, which can lead to vision loss (Hansen and Roach, 2006).

Radiation schemes are directed by the aim of treatment (palliative or curative), the type (benign or malignant) and location and extent of the tumour. The patient should be comfortable for the setup, which leads to greater reproducibility, and be appropriately immobilised. A GEC-ESTRO ACROP Guideline published in 2018 (Guinot et al., 2018) provides the latest recommendations for surface mould brachytherapy for skin lesions. The given fractionation schemes are:

1. 3 Gy per fraction, 17–18 fractions, 3 times a week, total dose 51–54 Gy;
2. 4 Gy per fraction, 10–12 fractions, 3 times a week, total dose 40–48 Gy;
3. 5 Gy per fraction, 10–12 fractions, twice a week, total dose 50–60 Gy or
4. 5 Gy per fraction, 8 fractions, twice a day, daily, total dose 40 Gy.

2.6 HDR brachytherapy dose calculations

Contemporary brachytherapy planning systems provide dose calculations by using the formalism of the AAPMs task group 43 report (Nath et al., 1995) and its amendment, (Rivard et al., 2004). The formalism, conventionally abbreviated

to TG 43, gives the dose rate $D(\dot{r},\theta)$ at a point P in the polar plane coordinate system in water, from the centre of a source with an air kerma strength denoted by S_K

$$\dot{D}(r,\theta) = \Lambda S_K \frac{G(r,\theta)}{G\left(1,\frac{\pi}{2}\right)} F(r,\theta) g(r) \tag{2.1}$$

where Λ is the dose rate constant, $\frac{D(1,\frac{\pi}{2})}{S_K}$ which equals the dose rate per unit air kerma strength U at one cm along a transverse axis of the seed in units $\text{cGyh}^{-1}\text{U}^{-1}$. The recommended Ir-192 value for Λ is 1.12 for a water medium. This comes from TG 43 update 1 (Rivard et al., 2004).

The Geometry Factor, $G(r,\theta)$, units cm^{-2}, accounts for the geometric fall off of photon fluence with distance from the source.

$F(r,\theta)$ is the anisotropy factor, normalised along the transverse axis, where $\theta = \frac{\pi}{2}$. This factor accounts for the angular dependence for photons that are absorbed or scattered in the medium.

$$F(r,\theta) = \frac{D(r,\theta) G\left(r,\frac{\pi}{2}\right)}{D\left(r,\frac{\pi}{2}\right) G(r,\theta)} \tag{2.2}$$

$g(r)$ is the radial dose function; it accounts for the radial dependence of photon absorption and scatter in a medium along the transverse axis

$$g(r,\theta) = \frac{D\left(r,\frac{\pi}{2}\right) G\left(1,\frac{\pi}{2}\right)}{D\left(1,\frac{\pi}{2}\right) G\left(r,\frac{\pi}{2}\right)} \tag{2.3}$$

If the source is approximated to be a point source, then the equation 2.1 simplifies to the following

$$D(r) = \Lambda S_K \frac{g(r)}{r^2} \phi_{an}$$

(2.4)

which introduces the new factor ϕ_{an} which is the distant dependent anisotropy factor. This factor gives the ratio of 4π as the average dose rate at a given distance which is divided by the dose rate at a point on the transverse axis of the source. For a radius of 1 cm the anisotropy factor is between 1.023 at 0 degrees and 0.9926 for 90 degrees for Ir-192.

Air Kerma Strength, S_K, is the unit of measurement recommended by the TG 43 amendment (Rivard et al., 2004). The brachytherapy source is the air kerma rate in free space times distance squared at the calibration point from the source centre along a perpendicular bisector

$$S_K = K_l l^2$$

(2.5)

and has units of μGym^2h^{-1}.

Air kerma strength is related to exposure via:

$$K = X \left(\frac{\bar{w}}{e}\right) \frac{\frac{\mu_{tr}}{\rho}}{\frac{\mu_{en}}{\rho}}$$

(2.6)

where K is kerma, X is the exposure, $\frac{\bar{w}}{e}$ is the average energy absorbed per unit charge of ionisation in air, $\frac{\mu_{tr}}{\rho}$ and $\frac{\mu_{en}}{\rho}$ are the average values of the mass transfer coefficient and the mass energy absorption coefficient in air for photons.

Also, $\frac{\mu_{en}}{\rho} = \frac{\mu_{tr}}{\rho}(1 - \bar{g})$ where $\bar{g}$ is the average energy lost by electrons due to bremsstrahlung radiation. For brachytherapy photons in air, $\frac{\mu_{en}}{\rho} \cong \frac{\mu_{tr}}{\rho}$ so

$$K = X\left(\frac{\bar{W}}{e}\right) \tag{2.7}$$

and

$$S_K = X_l \frac{W}{e} l^2 \tag{2.8}$$

Hence exposure calibration of brachytherapy sources can be converted to air kerma strength via equation 2.8.

If the exposure rate is defined in terms of R/h at a distance of 1 m, then

$$S_K = X\frac{R}{h}\left(0.876\frac{cGy}{R}\right)(1\text{m})^2 \tag{2.9}$$

where the value 0.876 is the value of $\frac{W}{e}$ for dry air.

The brachytherapy treatment planning system uses dose to water from each dwell position, pre-calculated using equation 2.1, and sums the dose from all dwell positions in the treatment plan using weightings for individual source dwell times.

Once the TG 43 methodology has been followed the treatment planning system interpolates dose calculation points to create a display of isodose curves around the source and dose volume histograms describing dose to the target and OARs. The main limitation of the TG 43 formalism is that this approach assumes the body is entirely water and has no corrections for tissue, scatter or source shielding. Other proposed approaches use Monte Carlo or linear Boltzmann

equation solvers (Petrokokkinos et al., 2011, Beaulieu et al., 2012) techniques. Of particular concern are shielding and scattering influences for skin and eye brachytherapy.

2.7 Limitations of HDR Brachytherapy Dose Calculations

The TG 43 formalism assumes that the irradiated volume contains only water and water equivalent tissues, TG 43 is therefore very useful for calculating dose in organs that contain and are surrounded by tissues with radiological properties similar to water, such as the prostate (Nath et al., 1995). Treatment planning systems that rely on TG 43 are, however, unable to account for the perturbations caused by high and low density media, such as bone (Beaulieu et al., 2012), metal shielding (Petrokokkinos et al., 2011), contrast media (Zhang et al., 2007, Bensaleh et al., 2009) and air gaps or 'missing tissue' (Mille et al., 2010, Pantelis et al., 2005, Kassas et al., 2006)

Beaulieu et al (2012) reviewed the literature comparing TG 43 data against more sophisticated methods such as Monte Carlo, and reported that TG 43 underestimates the dose to bone by up to 23%, due to both the density of the bone and its elevated effective atomic number, which leads to increased photoelectric interactions in bone. However, the studies they examined used relatively thick sections of bone for their calculations. For example, Anagnostopoulos et al., (2004) reported a 15% under dose in sternum bone, modelled as a 2.5 cm thick slab of cortical bone. Poon et al (2008) reported under doses of 18-23% in thick sections of pelvic and femoral bones. The potential inaccuracy of the TG 43 formalism, when calculating dose to the relatively thin orbit bone that lies close to the lower eyelid has not previously been established.

Several studies have investigated the effect of overlying air (known as missing tissue) on the accuracy of TG 43 calculations of breast brachytherapy dose (Mille et al., 2010, Pantelis et al., 2005, Kassas et al., 2006). Pantelis et al's (2005) results show an obvious dose depletion close to the surface of a spherical water

phantom, due to a lack of scatter from the air when an Ir-192 point source is placed at 2.5 cm depth. This dose depletion is not identified by the TG 43 calculation, due to the assumption that the patient is water, completely surrounded by water (Pantelis et al., 2005). Similarly, Kassas et al's (2006) results indicate that correction factors of 10% or more may be needed, to account for the dose-depleting effects of the air around the breast, when a balloon applicator is implanted within 1 cm of the breast surface. The possibility of correcting those effects using bolus or thermoplastic was not discussed by any of the authors (Mille et al., 2010, Pantelis et al., 2005, Kassas et al., 2006)

2.8 Verification of HDR brachytherapy dose calculations

2.8.1 Phantom measurements

In addition to performing independent dose calculations (as discussed in section 2.7), previous authors have also investigated the accuracy of HDR brachytherapy TPS dose calculations using experimental measurements.

For example, source calibration measurements are usually performed using ionisation chambers (Sarfehnia et al., 2010, Baltas et al., 1999). Two dimensional ionisation chamber arrays can also be used to evaluate HDR brachytherapy dose distributions (Manikandan et al., 2011), although such systems have low resolution (Spezi et al., 2005). Depth dose profiles (measurements of dose variation with distance from the source in water) have been measured using ionisation chambers (Rivard et al., 2006) and metal oxide semiconductor field effect transistors (MOSFETs) (Zilio et al., 2006). Point dose measurements around HDR brachytherapy sources have been performed using thermoluminescent dosimeters (TLDs) (Zhang et al., 2010, Kirov et al., 1995) diode dosimeters (Kirov et al., 1995) and MOSFETs (Qi et al., 2007)

All of the above dosimeters are limited by the ability to measure only point doses, 1D profile scans or low resolution 2D scans, and all of the above measurements were performed either in air, using purpose built jigs or in water (liquid or solid

phantoms) (Baltas et al., 1999, Spezi et al., 2005, Zilio et al., 2006, Zhang et al., 2010, Kirov et al., 1995, Qi et al., 2007)

By contrast, radiochromic film is a high resolution 2D dosimetry medium, which can be cut to size and used in heterogeneous, humanoid phantoms (Devic, 2011)

2.8.2 Radiochromic Film

Radiochromic film is an ultrathin colourless radiosensitive plastic approximately 7 - 23 μm thick with a radiosensitive leuco dye bonded to a 100 μm thick Mylar base.

The dye is polymerised by radiation exposure and it turns blue. The film has an almost tissue equivalency of 6 to 6.5 atomic mass units, compared to the effective atomic mass of tissue, 7.4. The radiation dose is measured by the optical density ratio,

$$OD = \log \frac{I_o}{I_t} \tag{2.10}$$

where I_0 is the amount of light collected without film, and I_t is the amount of light transmitted through the film.

Radiochromic film is self-developing and can be read on a conventional flatbed scanner however it does take several hours to have a stable colour change that is suitable for evaluation (Aland et al., 2011). The film works best just at or below 25 degrees Celsius and when it is not exposed to excessive humidity levels, and exposure to ultraviolet light can cause a colour change that is not related to the therapeutic ionising radiation. The optical density readout depends on the polarisation of light. It is best to use the same orientation for calibration and measurement (Aland et al., 2011)

Radiochromic film can be handled in the light, it can be cut and immersed in water and it is a valuable dosimetry technique for new conformal external beam radiotherapy techniques. There is a known variation in the response of radiochromic film, between the megavoltage and kilovoltage photon energy ranges (Butson et al., 2008, Peet et al., 2016). Since the mean energy emitted by the Ir-192 source is 380 kV, substantial corrections need to be applied if radiochromic film is used to measure HDR brachytherapy dose distributions after being calibrated in megavoltage external beam radiotherapy beams (Peet et al., 2016).

Radiochromic film dosimetry gives the spatial distribution of a dose in two dimensions and it is good for most radiation therapy uses because its composition comprises of 9% hydrogen, 60.6% carbon, 11.2% nitrogen and 19.2% oxygen, and its photon mass energy absorption coefficient and electron mass collision stopping power are similar to water and skeletal muscle. Radiochromic film is therefore close to tissue equivalent in the megavoltage photon range (Devic et al., 2005).

2.8.3 In vivo Dosimetry

In vivo dosimetry (IVD) enables measurement of radiation dose to patients during their treatment, thus ensuring the treatment plan is delivered as intended. In vivo dosimetry is considered an important part of quality management of a radiotherapy department, and is recommended by international organisations and guidelines such as the World Health Organization (WHO), the International Commission on Radiological Protection (ICRP) and the International Atomic Energy Agency (IAEA).

The AAPM TG 40 makes recommendations that in vivo dosimetry should be readily available for patient treatments to assure that there is a high maintained

accuracy in dose delivery (Kutcher et al., 1994). In vivo dosimetry is also a European Society for Radiotherapy and Oncology (ESTRO) requirement for external beam radiotherapy (van Dam and Marinello, 1994)

In vivo dosimetry is generally used for detection of gross treatment errors rather than for specific dose measurements. Theoretically, small dosimeters that are used in external beam radiotherapy are also suitable for use in brachytherapy. However, in vivo dosimetry in brachytherapy has several challenges compared to the flat dose profiles and homogenous dose in the target of external beam radiotherapy, mainly being the high dose gradients around the source.

One of the main advantages of brachytherapy, the steep dose gradients, can be problematic for in vivo measurements. Four millimetres from a line source the gradient is approximately 50% per mm, slowing to 6% per mm at a distance of 20 mm from the source, and 5% per mm at a distance of 35 mm, hence precise placement is important to obtain accurate results.

Detector energy dependence also needs to be taken into account, defined as the reading output from a detector as a function of absorbed dose in a medium on the energy spectrum. Most dosimeters exhibit a stronger energy dependence when used in brachytherapy than in a megavoltage beam. One of the main reasons for this is the greater dominance of photoelectric interactions causing an incorrect response. The absorbed dose sensitivity needs to be corrected if the dosimeter has been calibrated in a megavoltage beam.

Currently there are no ideal in vivo dosimeters for all brachytherapy measurements, although diodes, MOSFETS, TLDs, diamond scintillators and film have all been investigated for this purpose with varying degrees of success (Lambert et al., 2007, Therriault-Proulx et al., 2011, Toye et al., 2009, Pai et al., 1998, Alecu and Alecu, 1999, Haughey et al., 2011).

2.8.4 OSLDs for in vivo measurements

Optically stimulated luminescence dosimeters (OSLDs) have been reported as suitable dosimeters for in vivo measurement in a clinical radiotherapy setting (Jursinic, 2007, Dunn et al., 2013, Attix, 2008). In particular, Jursinic (2007) concluded that OSLDs offer many advantages over TLDs, including higher precision and accuracy in measuring dose, being small in size and having little energy (for MV energy range) and angular independence. OSLDs may replace both TLDs and diodes for in vivo dosimetry for routine clinical dose measurements (Jursinic, 2007). In fact, the Australian Clinical Dosimetry Service (ACDS) has deemed OSLD as a viable replacement for TLDs in their Level one audits nationally (Dunn et al., 2013).

The underlying physical principles of OSLD and TLD are comparable and well described by Attix (2008). Both dosimeters comprise a crystalline phosphor doped with an impurity that creates holes and traps electrons between valence and conduction bands during irradiation. Traps that hold the electrons within the gap vary both in depth and concentration. Trapped electrons may be optically (OSLD) or thermally (TLD) stimulated to emit optical photons upon electron hole recombination. The number of photons released is absorbed dose dependent.

Unlike TLD, which is stimulated by heat rather than light, OSLD offers a much faster readout speed and re-read capability. Jursinic (2007) described in detail the filter inside an OSLD reader. Key components include light source, photomultiplier tube (PMT) as well as the different filters used to discriminate between the light source used to stimulate the phosphor and the light emitted by the phosphor. Output pulses from the PMT are counted and displayed.

For use in a HDR situation, the OSLD needs to have an energy correction factor applied to the readout, as the OSLD does not behave in the same way as it would

under a 6 MV beam, due to the high effective atomic number of the OSLD (Yukihara and McKeever, 2011).

OSLD sensitivity when compared to 6 MV linear accelerator beams is between 1.25 and 1.1 This changes with the accumulated dose given to the dosimeter. Reported values of uncertainty when compared to dose calculations for brachytherapy range from -4.4 to +6.5% for skin dose. Some of the main characteristics that make OSLDs a good choice of dosimeter is their high radiation sensitivity, up to 60 times that of LiF TLD systems, low angular dependence, waterproofness and low volume averaging. Published values of the sensitivity adjustment can be used from OSLDs calibrated in a linear accelerator beam to mitigate the need for calibration in Ir-192 brachytherapy.

Because the use of superficial HDR brachytherapy with custom moulds is a new treatment for eyelid BCCs and SCCs, the use of OSLDs for in vivo dosimetry forms an important part of patient treatments. The main use for in vivo dosimetry in this case is to provide accurate readings for delivered dose to the lens and to monitor the treatment dose.

3. Patient Simulation and Brachytherapy Planning

3.1 Phantom and Mark-up

An Anthropomorphic stereotactic phantom, STEEV (Computerised Imaging Reference Systems Inc., Norfolk, USA) was used to mark clinically realistic BCC and SCC treatment areas on the lower right eyelid, as shown in Figure 3-1. The target was 40 mm long, 10 mm wide and 10 mm deep within the hypothetical right lower eyelid of the phantom.

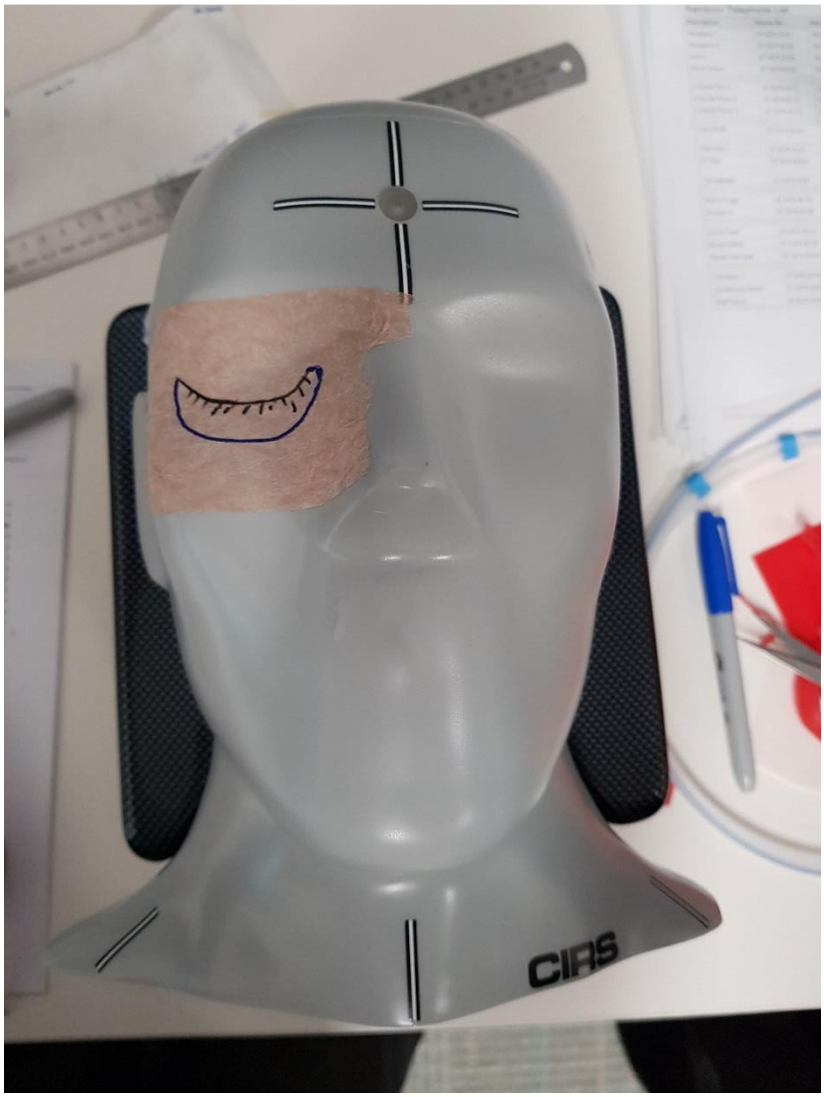

FIGURE 3-1 STEEV PHANTOM WITH OUTLINED LOWER RIGHT EYELID AND CLINICAL TREATMENT AREA

2 mm thick marker wire was used to outline the target volume and the phantom was CT scanned (Siemens Definition AS20 scanner) using the built in head

protocol (120 kVp, 165 mA and 0.6 mm slices) to assist with the eventual treatment planning. The wire was removed before catheter testing and mould construction, as the supplied x-ray marker wire was used for final simulation.

3.2 Catheter Selection

A 30 channel Elekta HDR remote Afterloader, Microselectron, (Elekta AB, Stockholm, Sweden) was used for delivery, using a single channel for the Ir-192 wire. The iridium source is 0.369 cm long and 0.065 cm high, encapsulated in a stainless steel capsule with wall thickness 0.02 cm. This is laser welded to a 0.07 cm thick source drive cable, 1.5 m long. (Islam et al., 2012)

Using the marked outline shown in Figure 3-1 as a guide, different brachytherapy catheter types and positions were tried to obtain optimal placement and coverage of the target region. Two catheter types were examined, the first being flexible catheters, (Flexible Implant Tube 6F, Elekta AB, Stockholm, Sweden) with the second being lumencaths (Lumencare Azure 6F, Elekta AB, Stockholm, Sweden). The features of these catheters are summarised in table 3-1. Flexible catheters were selected for testing due to their availability and use in treatments for superficial, breast and scalp. Lumencaths, which are conventionally used to perform treatments in lumens (mainly bile duct and bronchus) were observed to be thinner (1.6 mm diameter vs 2 mm for flexible catheters) and more flexible than the other catheters.

TABLE 3-1 PROPERTIES OF CATHETERS USED

	FLEXIBLE IMPLANT	**LUMENCARE AZURE**
KINK RESISTANCE	No	Yes
BENDING RADIUS	large	small
END BUTTON	Yes	No
INSERTABLE X-RAY MARKER WIRE	Yes	Yes
MULTIPLE USE (GENERIC USES)	Yes	No
LENGTH/THICKNESS	150 cm / 2 mm	150 cm / 1.6 mm
VENDOR	Elekta	Elekta

Catheters were tested by attempting to conform them to the surface of the phantom and checking for air gaps and overall flexibility and reproducibility.

The lumencath is generally used for a smaller number of fractions (see table 3-1) and the multiple uses required for SCC/BCC for this work required consultation with the manufacturer to ensure that the extended transfer use of the catheter would not result in any failures of the catheter, leading to emergency retrieval. This was also tested by running the check cable and live source cable through the catheter at least 80 times over the duration of 12 months. The lumencath was also exposed to heat from a water bath that is used to heat thermoplastics to 70°C, to see if the application of hot thermoplastic altered its effectiveness and dimensions. Higher temperatures were not tested due to there not being a situation where the catheter and thermoplastic would need to be heated above the water bath temperature.

3.3 Catheter Results

The standard superficial catheter shown below in Figure 3-2 was found to be unsuitable. There are large plugs at the end of the catheter, causing an unsuitably large gap between the catheter and the skin surface. These catheters are also relatively rigid, and not easily malleable to form a good contour of the treatment area.

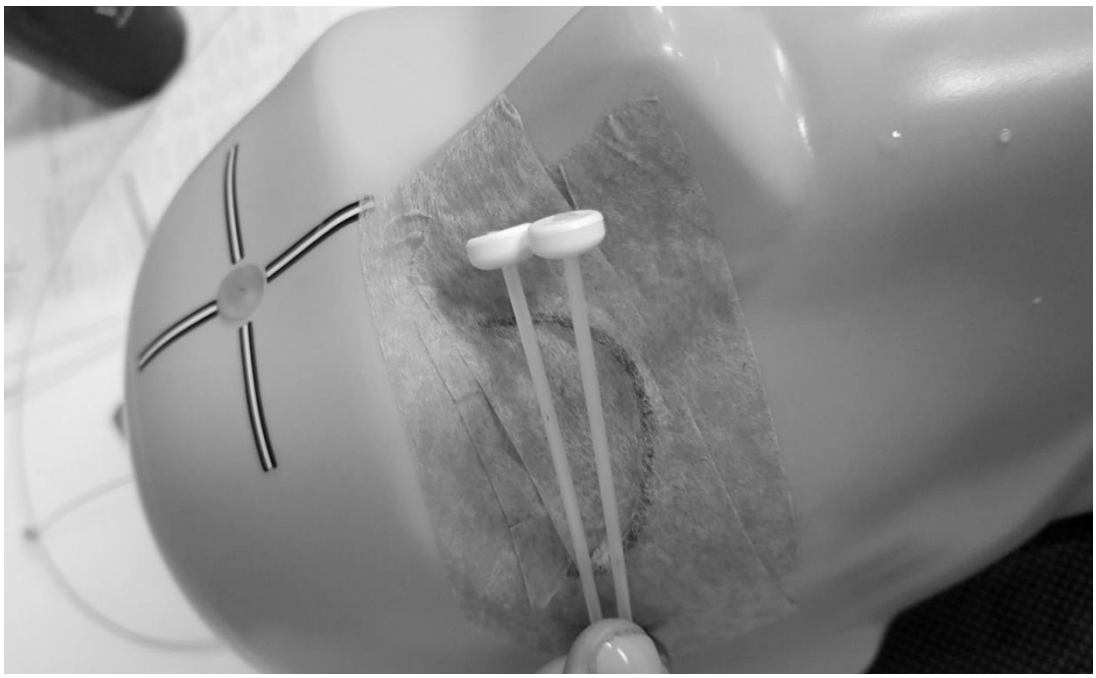

FIGURE 3-2 FLEXIBLE CATHETERS POSITIONED ON HEAD PHANTOM, SHOWING END PLUGS AND RIGIDITY

The second choice of catheter was the lumencaths, typically used for intraluminal treatments. These were found to have greater flexibility and were able to sit flat against the surface due to an absence of any bulky material at the tip of the catheter. These catheters had the added advantage of external markings showing the distance from the tip, to aid in treatment planning when used in conjunction with the x-ray marker wire, and to aid in placement of mould material. This catheter is pictured below in Figure 3-3.

FIGURE 3-3 STERILE BRACHYTHERAPY LUMENCATH WITH X-RAY MARKER WIRE

The results of additional testing, that was carried out after the lumencath was identified as preferable to the flexible catheter are summarised in table 3-2. These results confirm that the lumencath is suitable for use in delivering superficial brachytherapy treatments with a custom mould, despite not being designed for that purpose.

TABLE 3-2 TESTS AND RESULTS FOR CATHETER

TEST	RESULT
Suitability for delivery of multiple treatment fractions (query to vendor)	Correspondence confirmed this was OK
Suitability for delivery of multiple treatment fractions (repeated use)	Over 80 successful source and check cable test runs completed
Ability to withstand temperatures of 70°C without failure (water bath immersion)	Check and source cable test runs (above) completed successfully after heating and cooling of the catheter

3.4 Custom Mould Material Selection

Moulds of different materials were constructed and evaluated for their ease of use and repeatability as well as the ability to minimise air gaps between the catheter and the skin surface.

The first material used for a mould was red dental wax (Lordell Trading, Marrickville, Australia), 1.3 mm thick, softened and cut to outline the treatment area on the head phantom. Additional red wax was placed over the top of this, and secured with medical tape. This was to ensure that the catheter remained in position for simulation and treatment.

The second material used was thermoplastic (Action Products, Hagerstown, USA). This came in two forms, the first being small rectangular sheets, approximately 3 cm by 6 cm, and the other type were small 5 mm diameter spheres. They were both manipulated in a similar way, being heated in a water bath at approximately 70°C to soften them, until the thermoplastic became clear, and then either cut or hand pressed to make a mould surrounding the catheter, with the equivalent of one sheet thickness below the catheter and two above. This was further formed into the correct shape by placing it over the treatment volume on the eye and gently working into shape.

The two mould materials were tested using palpation and visual inspection. Variables evaluated were: the presence and extent of air gaps within the mould, the extent and reliability of contact between the mould and the phantom's surface, the amount of tape needed to fix the mould to the phantom, the stability of catheter positioning within the mould and the amount of tape needed to fix the catheter within the mould as well as ease of use.

Air gaps within the mould matter due to how the dose calculation algorithm works, and will introduce errors if there is air present due to the difference in density from water. The stability of the catheter position is important for geometric accuracy of treatment delivery (i.e. if the catheter moves, there is a potential for the target to be missed). The ease of use is of importance since there is the need to create the mould on the patient, so speed becomes important, also there is a need to be able to create a reliable mould thickness to ensure an accurate dose calculation.

3.5 Custom Mould Material Selection Results

The red wax was found to be hard to manipulate effectively into shape, and had air gaps when the catheter and additional wax was placed to hold everything together, see Figure 3-4. The use of substantial amounts of tape was also required to ensure that the catheter stayed still, which could lead to problems when cleaning between fractionations, and likely discomfort for the patient.

FIGURE 3-4 RED WAX ON PHANTOM, SHOWING GAPS AND POOR DELINEATION

Thermoplastic sheets were found to be the better option to create surface moulds. They were more malleable and can hold the catheter in a fully reproducible position using bony anatomy and the eyelid without the need for extra adhesive. The thermoplastic can be moulded to the surface of the eyelid prior to simulation. Figure 3-5 shows samples of thermoplastic being softened in the 70°C water bath. The thermoplastic is translucent when soft and turns white as it cools and hardens. The mould on the phantom can be seen in figure 3-7.

FIGURE 3-5 SOFTENING OF THERMOPLASTIC IN 70 DEGREE WATER BATH

3.6 Treatment Planning

The planning of a superficial treatment for the right eyelid target described in section 3.1 followed the general process used for interstitial treatment of eyelid carcinomas outlined in section 2.5 with the obvious exception that the catheter was embedded in thermoplastic and taped to the surface instead of being surgically implanted within the target tissue.

The catheter tip was placed on the right side of the phantom, with the remainder going over the forehead. The phantom was then scanned head first supine using the built in head protocol on the CT scanner, and exported to the Oncentra Treatment Planning system.

The CT scan of the phantom with thermoplastic and catheter and the CT scan of the phantom with wire markers only (see section 3.1) were both used to create treatment plans using the Oncentra Brachytherapy treatment planning system (Elekta AB, Stockholm, Sweden).

The eye lens, orbit and target geometry was defined by copying the shape of the marked area from the CT image with the wire marker onto the CT image with the catheter and then extending the volume to the required 5 mm treatment depth, as required by the radiation oncologist. The catheter was then digitised from the tip end with a minimum source step size of 2.5 mm, for the treatment length in both the sup and inf directions as given by the radiation oncologist. All dwell positions were activated and a set of three dose normalisation points were defined as shown by blue circles in Figure 3-6. Further information is found in Appendix B.

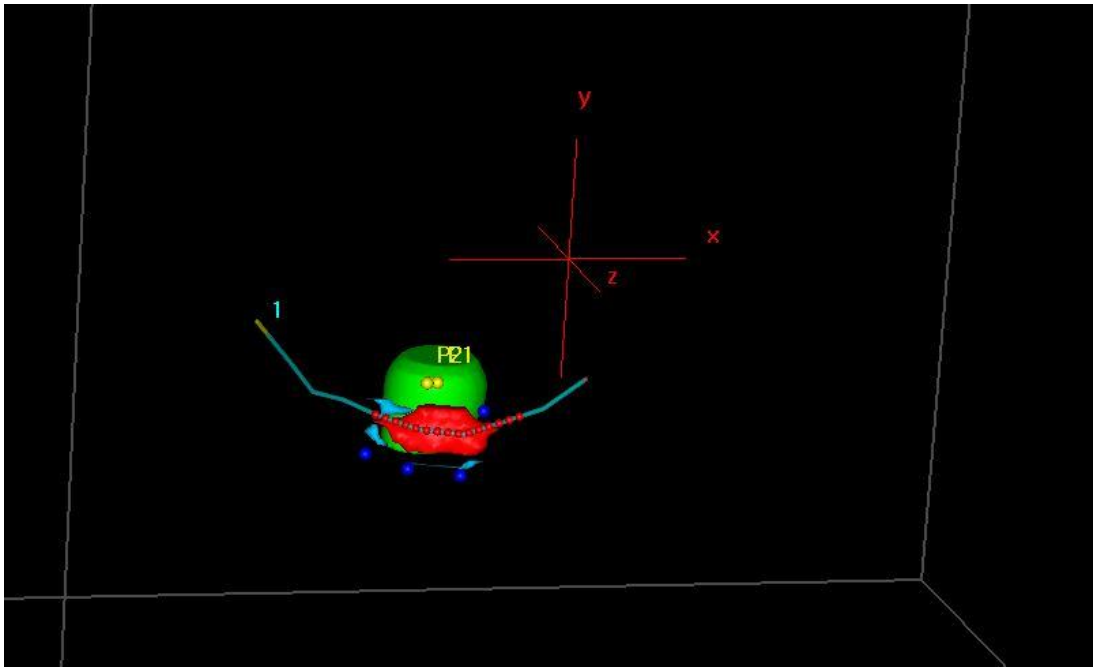

FIGURE 3-6 OUTLINE OF CATHETER IN ONCENTRA SHOWING DWELL POSITIONS IN RED AND NORMALISATION POINTS IN BLUE

A test prescription of 48 Gy to the treatment volume was used and dose was optimised to achieve a uniform dose to the PTV from the activated dwell

positions. Dose to OARs was checked and a Radiation Oncologist was asked to assess and approve the treatment plan.

3.7 Treatment Planning Results

Figure 3-7 shows the head phantom, with catheter and thermoplastic during the acquisition of the treatment planning CT images. The mould was found to be quite reproducible in setup location, the bony anatomy assisted by creating outside barriers for the mould to sit within, since the custom thermoplastic was being shaped to the area.

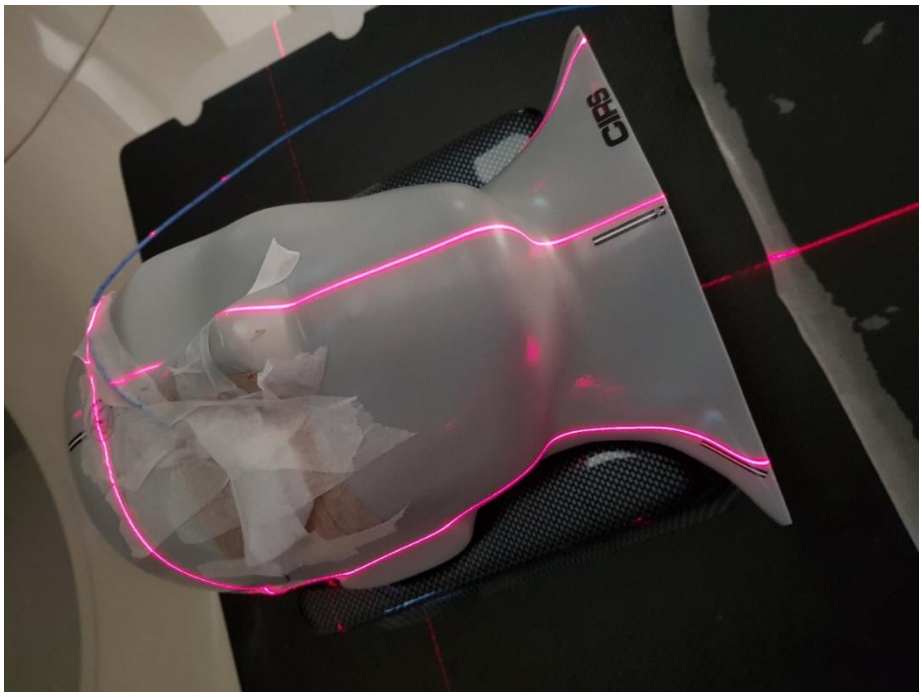

FIGURE 3-7 THERMOPLASTIC MOULD WITH CATHETER PRIOR TO SIMULATION CT SCAN

After plan creation, optimisation and final dose calculation, the 3D dose distribution appeared as shown in Figure 3-8 with the 100% dose cloud, shown in red, touching the points, in blue, in a 'sausage like' configuration. To achieve this uniform dose distribution, longer dwell times were used at the ends of the treated volume than in the central, curved region, as shown in table 3-3. Note that the dwell times listed in table 3-3 are relative to the dwell times used on the treatment day because the actual treatment time varies according to the date of treatment and the activity of the decaying iridium source.

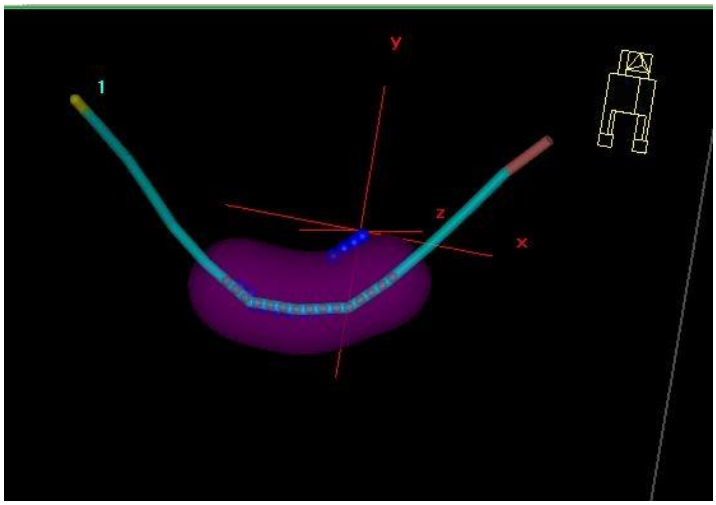

FIGURE 3-8 DOSE DISTRIBUTION FROM TEST PLAN. THE PURPLE SAUSAGE LIKE STRUCTURE SHOWS THE DOSE DISTRIBUTION AT THE 100% LEVEL, SURROUNDING THE BLUE DWELL POSITIONS

TABLE 3-3 RELATIVE DWELL TIMES USED IN TEST PLAN

POSITION	RELATIVE DWELL TIME
22	4.33
23	3.17
24	1.74
25	5.49
26	0.69
27	1.3
28	2.15
29	2.28
30	1.75
31	1.08
32	0.49
33	0.05
34	0.09
35	3.13
36	4.99

The isodose distribution shown in Figure 3-9 shows the steepness of dose falloff towards the eye, but also indicates the planning system has insensitivity to the

presence of air and other heterogeneous media. The shape of the dose distribution is determined only by the dwell positions, dwell times and the TG 43 model of the source, and not by any anatomical or density features of the phantom.

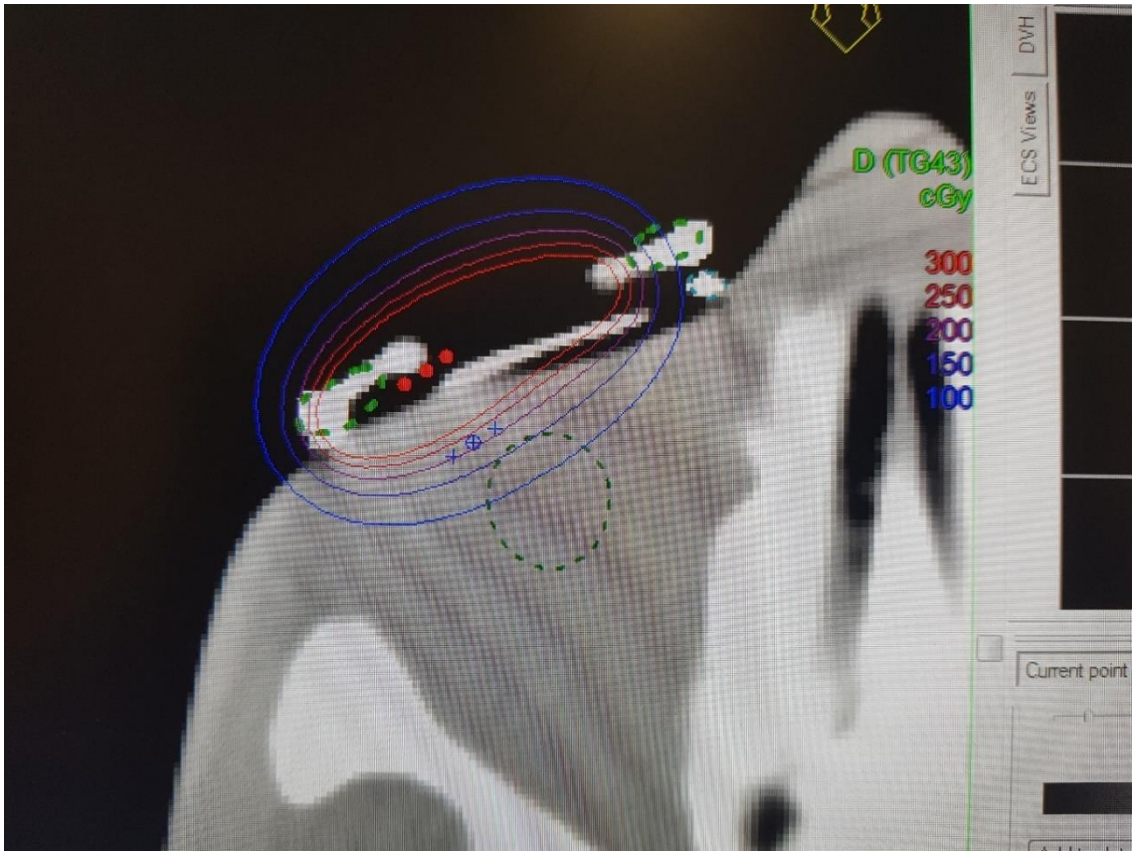

FIGURE 3-9 ISODOSE DISPLAY FROM RIGHT EYELID TEST TREATMENT PLAN WITH DOSE LEVELS OF 300, 250, 200, 150 AND 100 CGY

4. Film Measurements

4.1 General Method

Gafchromic EBT3 radiochromic film (Ashland Advanced Materials, Bridgewater, USA) was used to measure dose on and inside a head phantom, from the HDR brachytherapy treatment.

The film was analysed using a commercial software product, FilmQAPro film (Ashland Advanced Materials, Bridgewater, USA), following the instructions given by the manufacturer, which allowed the film measurements to be compared to an exported DICOM file from the treatment planning system.

The film was calibrated using a Varian Clinac, with a 10 cm x 10 cm field size, 100 cm SSD and 5 cm build up and backscatter. The monitor units delivered by the linac are displayed in Table 4-1, alongside the corresponding linac doses, where 1 cGy = 1 MU in a 10 cm x 10 cm field at 1.5 cm depth and the percentage depth dose value at 5 cm depth is 85.6%.

Table 4-1 also includes the doses that would have produced the same amount of film darkening if an Ir-192 HDR brachytherapy unit had been used to irradiate the calibration films, based on correction factors provided by Peet et al (2016)

TABLE 4-1 LINAC MONITOR UNITS AND CORRESPONDING DOSES FOR DIFFERENT BEAM QUALITIES

MONITOR UNITS	LINAC CGY	HDR CGY	CORRECTION
0	0	0	
20	17.12	19.34	1.13
50	42.80	48.44	1.13
100	85.58	96.49	1.13
140	119.82	134.1	1.12
190	162.61	180.46	1.11
230	196.85	216.8	1.10

4.2 Density Heterogeneity Effects

As established in section 2.7, one important limitation of the treatment dose calculation provided by the treatment planning system is the assumption that all

tissue is water. This poses a problem especially around the ocular region where a layer of bone approximately 6 mm thick (Xu et al., 2017) underlies the tumour. To investigate the potential dosimetric effects of this, density heterogeneity film was placed inside the head phantom, as shown in Figure 4-1 below.

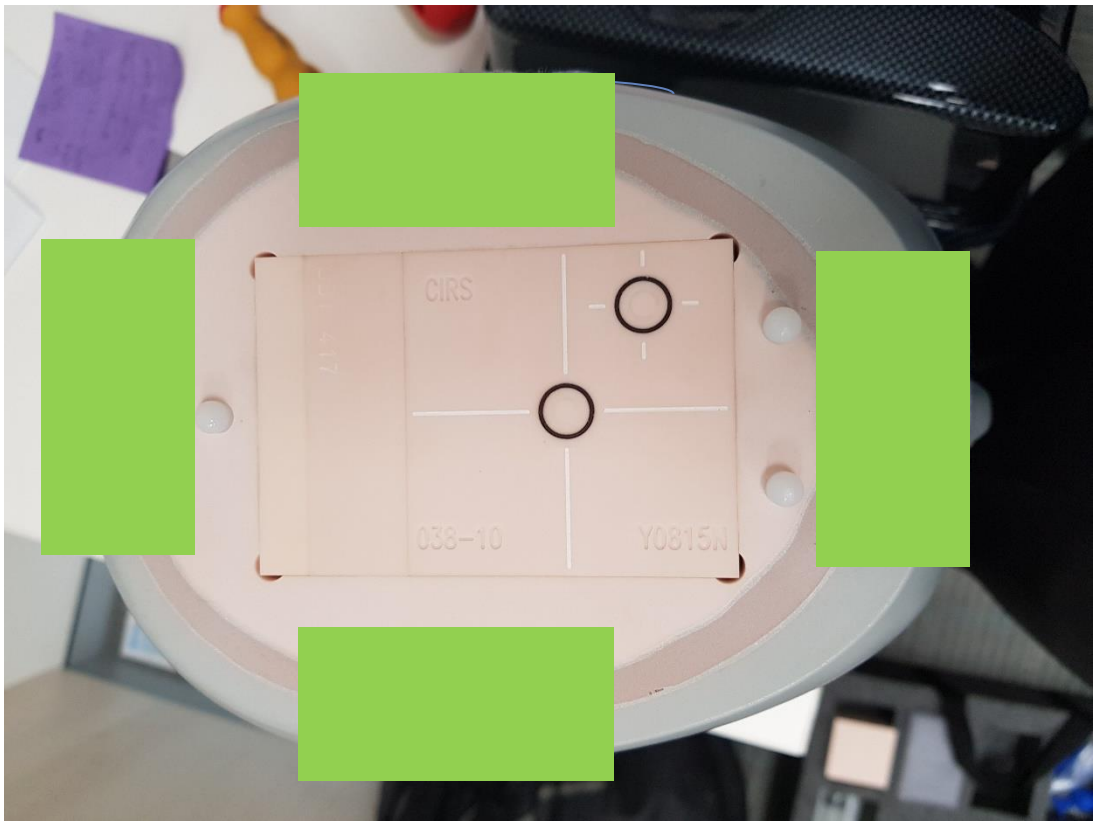

FIGURE 4-1 STEEV HEAD PHANTOM SHOWING BONE. FILM WAS PLACED SUP, INF, LEFT AND RIGHT ON THE EDGE, TO AT LEAST 5 CM TOWARDS THE CENTRE AS SHOWN BY GREEN RECTANGLES

The catheter was then run along the join perpendicular to each film position so that the effects of varying levels of tissue and bone could be measured and compared to a plan that was measured on a solid water phantom. A single dwell position dose of 2 Gy was carried out on film on one of the bone points to gain a depth dose for the source in bone, which was compared to the same single point 2 Gy fraction in a solid water phantom.

Four different locations with varying levels of skin and bone in the anthropomorphic head phantom were analysed, as well as a single point 2 Gy nominal dose delivered to one of these points, compared to a solid water slab, shown in Figure 4-2, note that different scales are used for the axis.

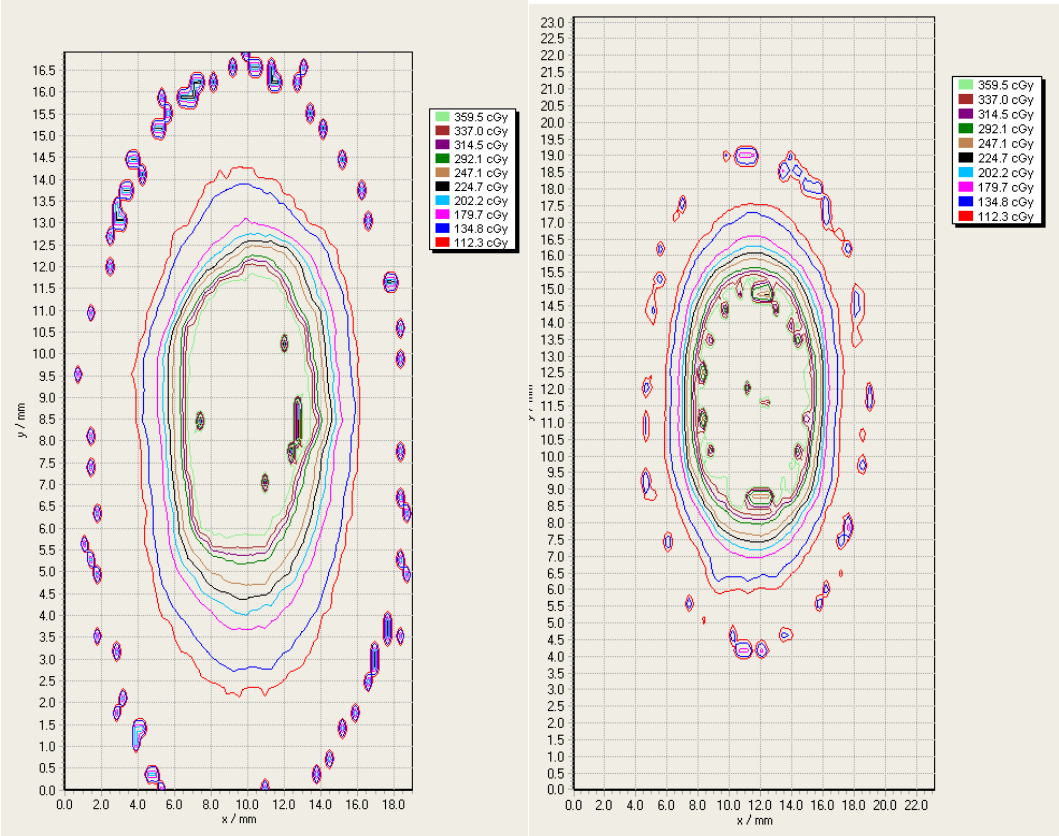

FIGURE 4-2 COMPARISON OF BONE DOSE (LEFT) AND SOLID WATER DOSE (RIGHT) FOR DELIVERED 2 GY, SHOWING FASTER ATTENUATION IN A HIGHER DENSITY MEDIUM (BONE)

This result, Figure 4-2, is a worst-case scenario resulting from measuring in thick bone, approximately 7.2 mm from the PTV, which is less relevant in an eyelid case however it provides a useful confirmation of the Monte Carlo results produced in the literature (Beaulieu et al., 2012). It shows that, as expected, there is a steeper dose falloff in bone compared to water due to the higher density of bone, so that the prescribed dose might not reach the complete depth of the tumour.

4.3 Missing Tissue Effects

As it is a superficial treatment method and the current dosimetry protocol used, TG43 dose calculation algorithm, assumes a water medium, different levels of bolus were used to try and simulate the differences between the body being assumed to be all water and the present situation of the catheter sitting on top of skin surrounded by air. This was done by placing the catheter on a solid water phantom with film inserted underneath the catheter and different levels of build up above the catheter.

The treatment plan was run through the catheter and the results analysed. In total there were 4 different levels of bolus used, 3 (the thinnest clinically available), 5, 8, and 10 mm. As misalignment of the proximal end of the profile had the potential to cause substantial uncertainties in the resulting measurements, due to the steep dose gradient adjacent to the source, particular care was taken to ensure each profile consistently started from the first pixel at the edge of the film. Further uncertainties (up to approximately 2%) may have arisen from small lateral displacements of each profile. The overall uncertainties affecting these measurements was dominated by scanning noise. Consequently, the film profile uncertainty is shown by the local dose variations (noise) in the profiles in figure 4-3 which have not been filtered or smoothed.

Results, as shown in Figure 4-3, suggest that any thickness of bolus ≥ 3 mm gives a dose distribution close to the 10 mm bolus dose distribution compared to treating without backscatter, shown by 0 mm bolus – catheter only. Enclosing the catheter in thermoplastic, with 6 mm of bolus backscatter provides a similar improvement. A thickness of at least 6 mm of thermoplastic above the catheter is therefore recommended when delivering HDR brachytherapy treatments to the eyelid. This holds for both high dose and low dose regions of the treatment plan PTV, as shown in (A) and (B) in figure 4-3. The dose difference of a profile between 10, 8, 5, 3 and 0 mm of bolus is shown in (C) and the difference between

10 mm (solid line) and other thicknesses is shown in (D). Figure 4-4 shows where the film profile was taken for a 'high' (in red) and 'low' (in blue) dose region of the plan. The films were overlaid in FilmQA Pro to match the isodose lines to ensure the correct placement of the profiles. In graphs A and B in Figure 4-3, differences decrease with increasing distance as the effects of phantom (patient) scatter overtake the effects of backscatter from the bolus.

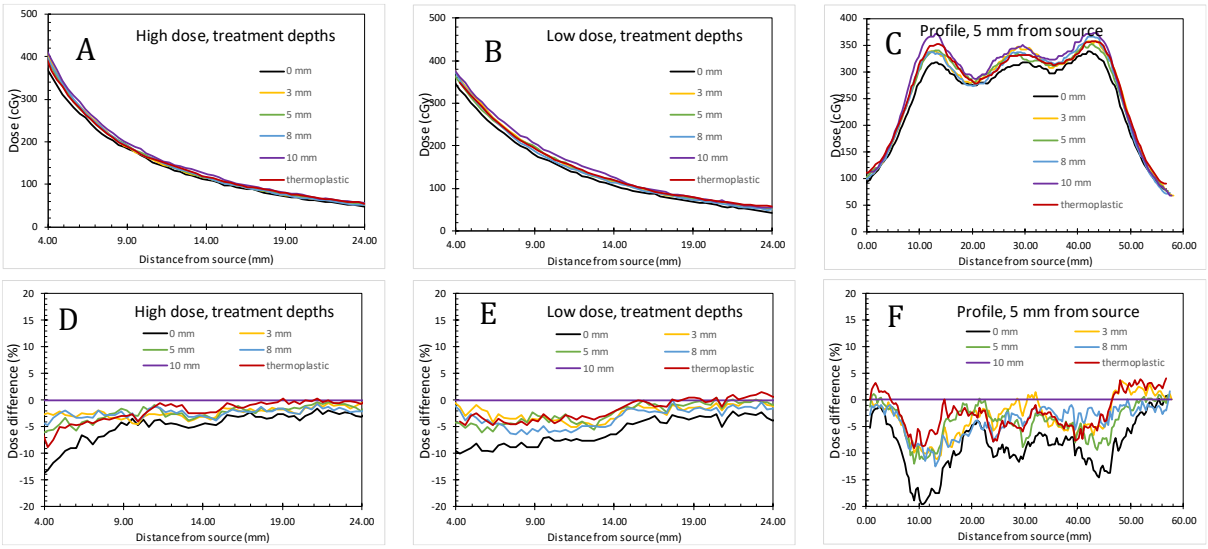

FIGURE 4-3 DELIVERED DOSE VS DISTANCE FROM SOURCE FOR FOUR DIFFERENT LEVELS OF BOLUS ON CATHETER. A AND B SHOW DOSE IN CGY AT DIFFERENT DEPTHS FROM THE CATHETER FOR A 'HIGH' AND 'LOW' DOSE REGION OF THE TREATMENT PLAN, C SHOWS A DOSE PROFILE 5 MM FROM THE SOURCE, D AND E COMPARE THE DOSE WITH DIFFERENT BOLUS LEVELS COMPARED TO 10 MM AND F SHOWS THE DOSE PROFILE COMPARISON TO 10 MM OF THERMOPLASTIC

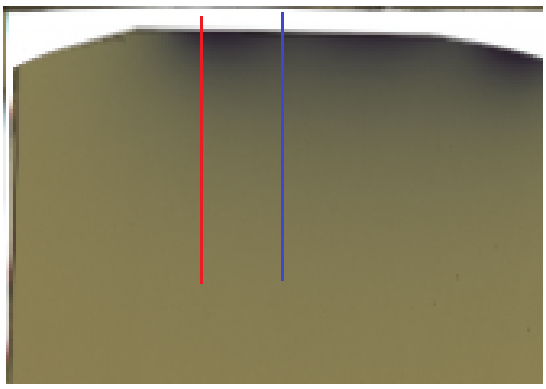

FIGURE 4-4 IMAGE OF SCANNED FILM SHOWING LOCATIONS OF 'HIGH' (RED) AND 'LOW' (BLUE) DOSE PROFILES

4.4 Lens Dose

Radiation induced cataracts are an important side-effect of radiotherapy treatments of the head (as discussed in section 2.5) and are of particular concern when treating regions close to the eye, such as the lower eyelid. Film measurements were used to evaluate the possible lens dose from a HDR brachytherapy treatment of the eyelid and investigate the possible benefits of placing lead shields directly over the eye orbit. External eye shields were chosen due to the availability in the clinic and the familiarity with these types of shields as apposed to an internal type shield which was unavailable and not used clinically due to the extra complexities and discomfort to the patient. An internal eye shield could also not be positioned on the phantom that was used. Two pieces of gafchromic EBT3 film were analysed to ascertain the eye lens dose for the created brachytherapy treatment plan. The films were placed on the outside of the STEEV phantom, covering from the base of the eye mould up to the top of the orbit. These doses were measured in two separate ways; the first was with the lead lens shield present on the head phantom and the second without. The lead shield was approximately 5 mm thick covered with a layer of adhesive tape to prevent direct contact between the patient's skin and the lead. By using the radiochromic film a dose distribution showing the dose over the entire orbit location can be analysed.

From Figure 4-5 it can be seen that without the lead eye shield the total dose to the eye lens of 24.2 Gy is approximately 50% of the prescribed dose. When the lead shield is placed on the phantom the eye lens dose in the same position as shown in the graph below is calculated at 37.5% of the prescribed dose, or 18 Gy in total.

The lines shown in Figure 4-5 illustrate the variation in dose across the eye region. From this it can be seen that if the eye lens is placed approximately 5 mm superior to the centre of the orbit the eye lens dose can be reduced to 1.8 Gy total, in conjunction with the lead eye shield. Without the eye shield the dose would be

15 Gy, at the same location. Patient coaching would be required to obtain this result.

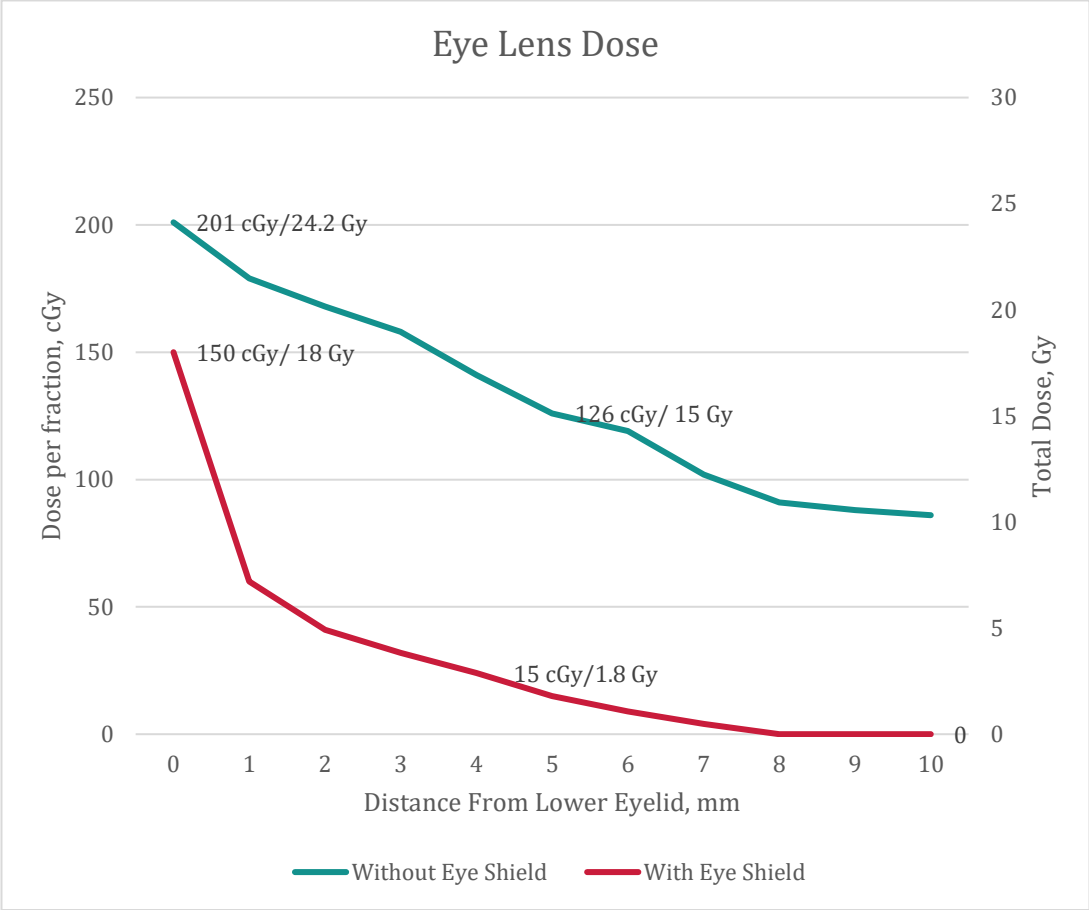

FIGURE 4-5 DOSE TO SURFACE OF EYE, MEASURED WITH AND WITHOUT EYE SHIELD, USING FILM WITH SINGLE FRACTION SCALE ON THE LEFT AND TOTAL DOSE ON RIGHT AXIS

These results show that treatment in this area may lead to significant unavoidable doses to the eye lens. This is why an ophthalmic review is strongly suggested and the patient is aware of any side effects and of those side effects which can be treated post radiation therapy, so that they can provide informed consent for treatment. It is also to be noted that the cohort of patients will most likely develop some of these complications regardless of radiation treatment due to age, as discussed in section 2.5.

5. OSLD Measurements

5.1 Overview of OSLDs

5.1.1 General Method

The OSLD system used in this work consisted of 25 OSLDs (Landauer Inc., Glenwood, USA). Each OSLD is comprised of a carbon doped aluminium oxide (Al_2O_3:C) compressed powder, pressed into a cylinder inside a square light proof plastic housing. The powder and plastic housing together will be referred to as OSLDs throughout this thesis.

The reader system comprises a MicroStarii InLight reader connected to a laptop hosting the required software. Each OSLD housing has a unique QR code with the serial number and specific sensitivity of the powder, which is read into the system using a built in laser barcode reader.

Initial verification of the OSLDs was carried out using an external beam radiotherapy system, in order to achieve a consistent and uniform dose readout between and within the OSLDs. The OSLDs were irradiated using 6 MV photon generated by a Varian Clinac iX series Linear Accelerator (Varian Medical Systems, Palo Alto, USA).

Standard grade solid water was used for both build up and backscatter in this study. Thin bolus was used to cover the OSLDs. The aim of the bolus was to eliminate the air gap created by the casing of the OSLDs and thus provide adequate lateral scatter equilibrium to the sensitive volume.

A Farmer type cylindrical ionization chamber and a Markus parallel plate chamber (PTW-Freiburg, Freiburg, Germany) were used with the Wellhofer dosimetrie Dose 1 (IBA dosimetry, GmbH, Schwarzenbruk, Germany) electrometer to determine the dose output (cGy/MU) in solid water for the 6 MV photon beam.

To generate the low dose calibration for initial verification, OSLDs were exposed to 0, 1 and 5 cGy and for the high dose calibration the OSLDs were exposed to 0, 50, 150 and 300 cGy.

The relevant output factors and depth dose corrections were applied. Finally, using the above method two QC OSLDs were created for low (3 cGy) and high (200 cGy) doses. The QC OSLDs were used to confirm accuracy of the calibration curve. The dose determined by the QC OSLDs was expected to be within 2% of the exposed dose level.

To use the OSLDs in brachytherapy energy qualities, a conversion factor published by Jursinic (2007) was used. This converts an OSLD calibrated in 6 MV megavoltage photons to enable it to be used for HDR brachytherapy using Ir-192. The OSLD over responds in a HDR situation by a factor of 1.06. This published correction factor was subsequently used.

5.1.2 Initial Verification of OSLD System

The physical dimensions of all OSLDs were inspected by observation, followed by measurements using a Vernier calliper of 30 OSLDs as a sample. Subsequently, the centres of the OSLD sensitive volumes were determined as discussed in section 5.2.2.

The integrity of the microStarii reader was tested by taking 20 repeated measurements as part of an intrinsic measurement test. The results of this test were compared against the results of the same test carried out at the Landauer factory prior to shipping.

Following the procedure detailed on the Landauer's "Calibrating the microStar" document (Yahnke, 2009), the tests summarised below as recommended by Yahnke has been used to establish the intrinsic precision of the reader, by checking the provided high dose quality control OSLD for reading reproducibility.

The quality control dot was scanned using the QR code scanner, placed into the reader barcode side up and then automatically read ten times by the reader. A pass result is when the coefficient of variation of the OSLD readout is less than one percent.

The 250 screened OSLDs were exposed to 2 Gy under 600 MU/min, 6 MV photons and a 10 cm x 10 cm field size at 15 mm depth. All OSLDs were read at least five times (Bell, 1999) or until reading becomes stable to determine the reproducibility of the OSLD readout, repeated readings reduce the inconsistency caused by operator error and/or the reader. An element correction factor (ECF) for each individual OSLD was determined thereafter using the following equation:

$$ECF = \frac{Individual\ nanoDot\ reading}{Delivered\ dose} \tag{5.1}$$

A review of previous studies (Jursinic, 2007, Dunn et al., 2013, Attix, 2008) revealed that shallow traps give rise to unstable luminescence at ambient temperature as trapped charges may be released after a short period of time even without stimulation (fading effect), e.g. TLD (LiF) of >20 hr has been reported as a practical time in a clinical setting (Kron, 1994). The same phenomenon was tested for the OSLD system with a waiting time of $>$ 10 minutes.

Most trapped charges in an OSLD remain bound after initial measurement due to both short stimulation time and low light intensity used within the reader for dosimetry purposes in radiotherapy (IAEA, 2013). Yahnke (2009) referred to this effect, and states that each analysis consumes only ~0.25% of the stored charge when using the strong beam, or ~0.04% when using the weak beam.

In this study, OSLDs were read at 3 minute intervals over a period of 33 minutes in order to provide an optimal post irradiation time for the dosimeters to reach stability. Each OSLD was then measured continuously over four minutes with no time delay between reads.

5.2 OSLD Measurements

5.2.1 Initial verification

The coefficient of variation (CV) specified by the vendor over 10 readouts of a single OSLD is 1%. The test results determined the CV to be 0.57% and thus within specification. This confirms that both the signal output and the mechanical integrity of the reader are in good condition.

The physical dimensions of the OSLDs were measured to be within the specifications provided by the vendor as illustrated in Figure 5-1. Reading error for the Vernier calliper is established at $\pm$0.05 mm, which includes the limitation of the calliper scale, as well as human error. The overall width of the OSLD is 10.1 mm including an extension of 0.5 mm.

The location of the sensitive volume of the OSLD inside the casing was also determined. The bottom image in Figure 5-1 indicates that an approximate distance ratio of 6:4 has to be accounted for. Measurements were performed on 30 samples and a variation of approximately $\pm$0.02 mm was observed in both width and length; the thickness was consistently 2 mm as specified.

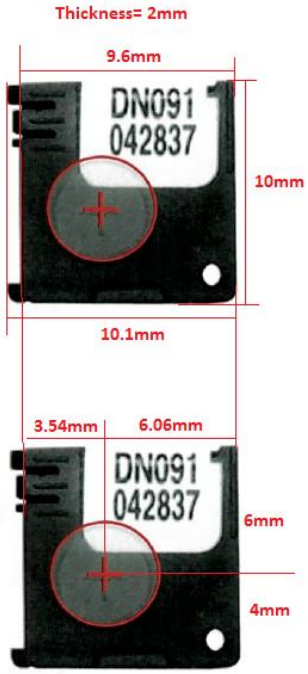

FIGURE 5-1 PHYSICAL DIMENSIONS OF A SINGLE OSLD, IMAGE FROM MANUFACTURER

5.2.2 Acquisition of calibration curve and production of quality control (QC) dosimeters.

The dose output (cGy/MU) measured immediately prior to the OSLD calibration was 1.0023 (± 3%) for 6 MV photons. A 15 mm build up was used on top of the OSLDs for 6 MV while 20 mm build up was used for 9 MeV. Assuming that the sensitive volume of the OSLDs is sandwiched between the black casings, the radiation depth would be increased by 1 mm.

For 6 MV photons, the PDD curve shows that d_{max} is 14.9 mm; hence the use of 15 mm of solid water will only require minimal correction. On the other hand, 20 mm build up used in 9 MeV plus 1 mm to the sensitive volume means a correction has to be applied to obtain relative dose at d_{max}, which is 19.1 mm according to the latest annual QA data (GenesisCare, internal report). Table 5-1 shows the final values used in the calibration curve for 6 MV photons.

TABLE 5-1 VALUES INPUT INTO MICROSTARII SOFTWARE TO CREATE A CALIBRATION CURVE

		6 MV
	Total Factor	0.9977
	MU applied	
HIGH DOSE	50	49.9
	150	149.7
	300	299.3
LOW DOSE	1	1.0
	5	5.0

In relation to the build-up used for calibration, it was questioned whether an additional 1 mm of build-up should be considered due to the location of sensitive volume of the OSLD sandwiched within a 2 mm thick casing, contributing additional plastic and small air gap. Based on commissioning data, a 1 mm differential would result in a dose variation of 0.15% for 6 MV photons. Moreover, uncertainties within the calibration process arise between exposures to the OSLDs at d_{max} against the ion chamber at d_{10} (to minimise electron contamination at d_{max}). However, OSLD detectors used clinically will likely to be affected by electron contamination to a similar magnitude so the extra 1 mm of build-up was not taken into account.

QC dosimeters of 200 cGy and 3 cGy were also tested against the two calibration curves created. Measurement results were within 2% of the exposed dose level for both curves. This is as expected; Jursinic et al (2007) have shown that OSLD exhibits little to no energy or modality dependence.

Delivery of known doses of 200 cGy resulted in an average reading of 201.76 cGy with 2 standard deviations of 6.96 (95% confidence) and CV of 0.03%. Figure 5-2

shows the distributions of ECF from the OSLDs measured. In this test, ECFs were determined to be minimal, with the mean readout standard deviation of 0.017%. In contrast Dunn et al, (2013) using 1562 OSLDs for a national dosimetry audit found a standard deviation of 0.640%. In a clinical setting however, given the external factors of uncertainties including patient movements, accuracy of dosimeter's location amongst others, ECF application may not to be necessary, or perhaps a batch rather than individual ECF could be used given the little variation in correction.

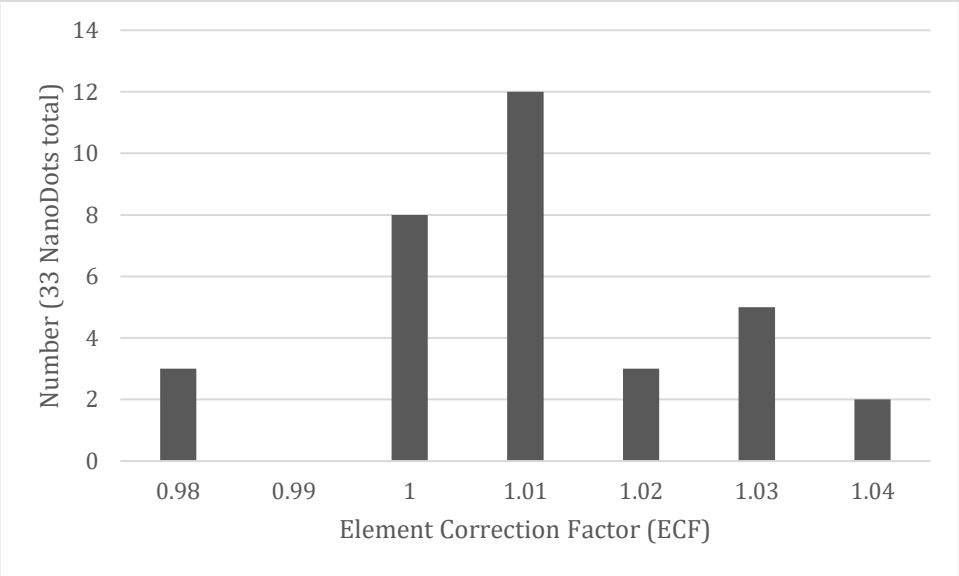

FIGURE 5-2 ECF (AVERAGE/DOSIMETER RESPONSE) DISTRIBUTION FROM A SAMPLE OF 33

Figure 5-3 shows the trend of the fading effect, normalised to 20 minutes. Initial transient signal decay was observed between 3 - 6 minutes post irradiation followed by relatively consistent readouts. The time (30 minutes) chosen represents an approximation of a practical time frame achievable in a clinical setting between in vivo measurements and obtaining a read out. The initial depletion trend shown in figure 5-3 agrees with the literature (Dunn et al., 2013, Jursinic, 2007), where no noticeable change in signal was reported between 15 minutes up to hours and even days after it has reached stabilisation.

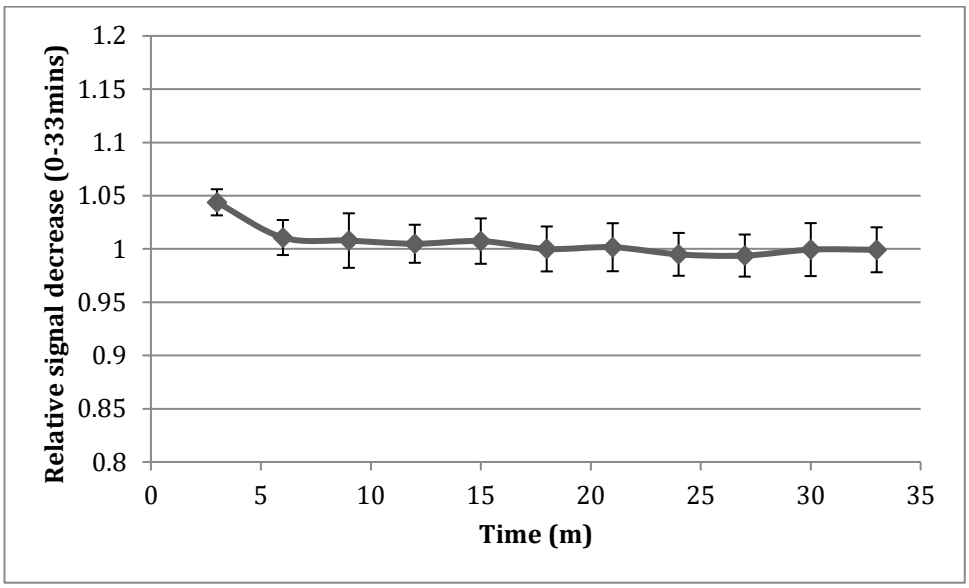

FIGURE 5-3 SIGNAL FADING OF 3 DOTS AVERAGED OVER 33 MINUTES, ERROR BARS DEPICT CV OF 3 DOSIMETERS

In contrast to a TLD system, OSLD not only reduces the waiting time between irradiation and measurement by ~1 day, it also allows repeated measurement, thus dosimeters may be retained as a record if necessary, to then be re-examined should there be any uncertainty or dispute.

Figure 5-4 shows the averaged dose response for each of the OSLDs tested and it demonstrates reasonable linearity with a slight increase of 0.006 to 0.035 (two standard deviations) as the dose begins to accumulate from 40 cGy to 200 cGy. Other studies had demonstrated that the dose response is supralinear, with the degree of supralinearity being dependent on the accumulated dose (Dunn et al., 2013). The dose range tested was 0-1100 cGy. A total dose of up to 200 cGy delivered at 400 MU/min (40 cGy per beam) was used to simulate a typical IMRT/VMAT treatment as this is more relevant in a clinical radiotherapy setting. The 40 cGy increments, accumulating to 200 cGy, as shown below in Figure 5-4 were measured to be 39.90 $\pm$ 0.01 cGy; 79.73 $\pm$ 0.02 cGy; 120.89 $\pm$ 0.02 cGy; 162.53 $\pm$ 0.03 cGy and 204.34 $\pm$ 0.03 cGy consecutively with 2 standard deviations for the 3 repeated measurements, excluding calibration error and ECF. Dose rate independence of OSLDs has been established in the literature

(Jursinic, 2007). This is relevant for Ir-192 as the dose rate effectively decreases as the source ages.

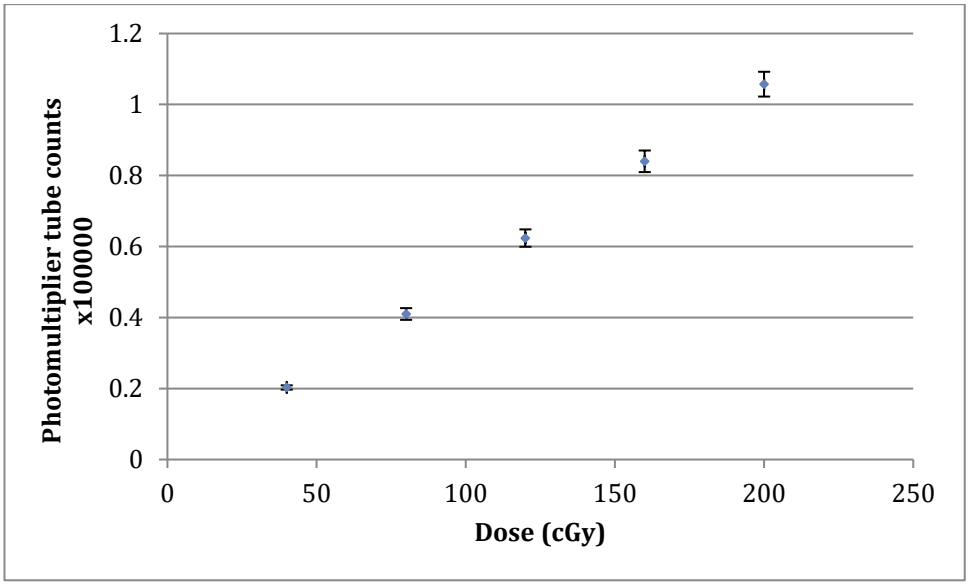

FIGURE 5-4 DOSE RESPONSE AVERAGED OVER 40 CGY ACCUMULATED DOSE UP TO 200 CGY 2 SD ERROR BARS

5.3 In vivo Measurements

5.3.1 OSLD Measurements of Treatment Dose

After establishing the accuracy and reliability of the OSLD system, a series of OSLD measurements of the surface dose on the head phantom was completed, using the test eyelid treatment plan described in section 3.4.

The OSLD measurement locations on the phantom head that were used to obtain some surface dose measurements are shown in Figure 5-5.

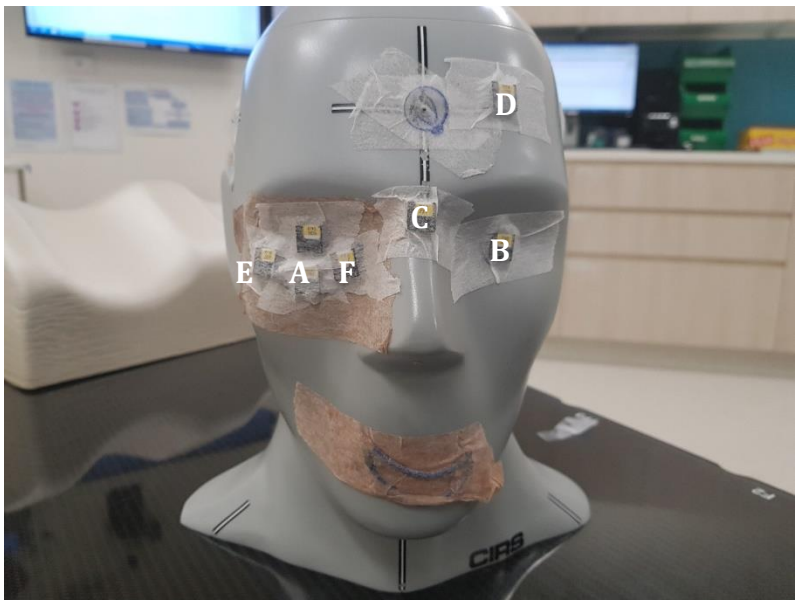

FIGURE 5-5 OSLD LOCATIONS ON STEEV HEAD PHANTOM

The positions shown in Figure 5-5 were chosen for clinical relevance, showing the dose to the target (A), the eye lens dose for both eyes (B), the nose dose (C), the transit dose of the source across the forehead (D)

OSLD measurements at positions around the ocular region (labelled A in Figure 5-5) were completed in combination with film measurements, to investigate whether in vivo measurements using OSLDs could be used to verify the accuracy of treatment delivery. OSLDs have some limitations when used close to HDR brachytherapy sources. The sensitive volume is a disc, so it is highly vulnerable to the steep dose gradients present in HDR treatments. OSLDs were placed at several distances from the source to ascertain the optimum minimal distance for accurate measurements. The effective point of measurement of the OSLDs, 1 mm, was taken into account when collecting the relevant TPS data for each location.

Film and OSLDs were placed over the eye lens in different locations, labelled B in Figure 5-5, to determine the lens dose and this was compared to the brachytherapy planning system dose.

The dose to the centre of the nose (labelled C on Figure 5-5) was also measured to help ascertain the TPS calculation of dose falloff with distance.

A measurement was also done on the forehead, labelled D in Figure 5-5, due to location of the catheter. It is necessary due to the mould placement for the transfer cable to traverse the head. Due to the speed of the source deployment there would not usually be any dose associated with the transit however this was still quantified.

5.3.2 Treatment dose measurements

Table 5-2 shows the results of OSLD measurements on the surface of the head phantom during the HDR treatment of the right eyelid. These results were compared to the treatment planning system dose and a film measurement (the circular ROI on the film analysed was the same as the Al_2O_3:C compressed powder disc size in the OSLD) in the same location. Film results at points far from the PTV agree within experimental error with OSLD results, negative film dose at B were excluded. Film and OSLD agree within experimental uncertainty for the Central and Left portions of the PTV. For the Right portion PTV, the discrepancy is on average 13% lower for the OSLDs. Film measurements agree with TPS values within experimental error. This shows that OSLD measurements can be used appropriately to estimate dose for brachytherapy treatments in low dose gradient regions, which are far from the PTV. It is not appropriate to estimate dose using the TPS for areas far from the PTV due to the TPS calculation algorithms used (Rivard et al., 2004).

TABLE 5-2 OSLD, FILM AND TPS DOSES, IN CGY, FOR GIVEN AREAS OF INTEREST, AND 95% CONFIDENCE INTERVAL RANGE

LOCATION (SEE FIGURE 5-5)	OSLD (95% CI)	TPS	EBT3 FILM (95% CI)
CENTRE L FOREHEAD (D)	0.97 (0.92-1.02)	0	1.1 (0.67-1.44)
R SIDE OF PTV (E)	412.6 (392-433)	474	472 (462-481)
C PART OF PTV (A)	335.2 (318-352)	348	356 (348-363)
NOSE TIP (C)	1.85 (1.76-1.94)	1.02	1.43 (1-1.86)
L EYELID (B)	0.5 (0.47-0.53)	0	0.26 (0-0.69)
L SIDE OF PTV (F)	472.8 (449-496)	459	480 (469-489)

There was no statistically significant difference to the dose count readout when the OSLD was exposed to the same 200 cGy dose, where one was submerged in the 70°C water bath (204 cGy) and the other was kept dry (202 cGy). This shows that in vivo measurements can be taken inside the mould without affecting the dosimeter, as to create the mould the thermoplastic can reach up to 70°C.

The dose to the normal resting location of the eye lens can also be calculated by the use of the OSLDs. These reading showed a dose of 1.4 Gy per fraction when the eye is in its normal location with the eye shield, and approximately 2 Gy without the eye shield giving a reduction of 28%. This is slightly different to the level measured with the film, being 2.02 Gy without the eye shield and 1.5 Gy with the shield. The difference in measurement values between the two techniques however is within the experimental uncertainty.

From this a conclusion can be drawn that if the patient were to use a lead eye shield the lens dose would be reduced which will lead to less side effects.

5.3.3 Use of OSLD as an Invivo dosimeter

The use of radiochromic film to evaluate HDR brachytherapy dose is relatively well established (see section 2.8.2) compared to the use of OSLDs for this purpose (see section 2.8.4) Therefore, before accepting OSLDs as a suitable in vivo dosimetry system, it was important to verify the OSLD measurements using radiochromic film measurements.

For comparison of OSLD to film there were two different configurations used, the first with the OSLD placed on top of the film and the second configuration had the OSLD placed underneath the film. The locations on the phantom were the same for both setups. Film was also used over the eyelid to provide a gradient dose for the lens depending on where the patient is looking at the time of treatment. This was previously shown in figure 4-5.

The results of placing OSLD and film together on the surface of the phantom showed that when the film was under the OSLD and the catheter the dose was more blurred on the film, resulting in a difference of 21.5% per fraction compared to having the OSLD under the film in the same location but on separate occasions. This can be attributed to the OSLD causing perturbation of the radiation field and leading to an erroneous dose on the film. This leads to the recommendation that OSLDs can be effectively used for OAR (in this case, eye lens) monitoring, however should not be used in the direct path of the Ir-192 source, therefore the poor agreement of the data in table 5-2 between OSLDs and film does not have any clinical consequences.

The total transit dose from the source travelling across the forehead summed for all fractions was found to be 9.3 cGy. It was measured to ensure the optimum placement of the catheter does not need to be readjusted due to the catheter travelling large distances across the skin. Due to the speed of the source it is confirmed that this dose is negligible.

5.4 Development of in vivo dose measurement technique

Of concern in radiation therapy is the dose to healthy organs surrounding the tumour site. The main organ at risk for lower eyelid brachytherapy is the lens of the eye area being treated. In consultation with a radiation oncologist the eye lens doses should be minimised. However, if it is known that due to the close proximity to the tumour there will most likely be a significant dose to the eye lens then there are mitigating steps that can be taken post treatment to ensure their side effects are minimised. In vivo measurements of lens dose can produce important information, to help guide clinical decision making after the treatment commences. These measurements are especially important for the early eyelid carcinoma cases, when the HDR brachytherapy treatment process has been newly introduced.

Information obtained from the measurements described in chapter four and five was used to design a proposed in vivo dosimetry process, using OSLDs, during superficial HDR brachytherapy treatments of eyelid carcinomas.

5.5 Proposed in vivo dosimetry system

As the method discussed is a new type of treatment, in vivo dosimetry plays an important role in the execution of treatment. It is recommended that a calibration be performed on the OSLDs under a linear accelerator, and response corrections be applied (in this case, divided by 1.06 as mentioned above in section 5.1.1) rather than direct calibration in a brachytherapy situation. It is far simpler to set up the calibration using a linear accelerator and easier to reproduce the scenario without added sources of error such as a decaying source and the rapid fall-off from an Ir-192 seed.

It is recommended to expose at least two OSLDs to a known dose of 0, 50, 100 and 300 cGy, by placing at least 10 cm of backscatter and 1.5 cm of build-up on the couch. The correction factor of 1.06 for dose should be applied before inserting them into the microstarii to generate a calibration curve. These corrected doses are to be used in the software input for dose.

Once the curve has been established, the OSLDs from a brachytherapy treatment can be analysed without any further setup. The use of OSLDs is far quicker than the use of film, as an individual calibration does not need to be performed. The readout of dose can take place within 10 minutes of exposure, whereas film has to self-develop for 24 hours before being analysed, based on current departmental protocols. This means that if there is something abnormal in the dose, it can be rectified faster with the use of OSLDs. OSLDs can also be kept for readouts in the future, and can be stored without loss of signal.

The OSLDs on the patient should not be placed directly under the surface mould or catheter. This is to ensure that the positioning of the OSLDs does not make the plan deviate from the calculated doses. The predicted dose from the treatment planning system should be known to form a comparison to the measured doses.

It is recommended that in vivo dosimetry be performed at least on the first fraction of treatment, and as regularly thereafter as the radiation oncologist prescribes. Any major deviations from the planned dose should be investigated, especially to known organs at risk.

The OSLD should be affixed over any film that is being used concurrently, and does not need to have any additional build-up attached, and can be easily secured with medical tape.

The most important location for the OSLDs in this case is the eye lens to measure lens dose.

6. Discussion

This thesis describes the development and evaluation of a superficial HDR brachytherapy treatment technique for lower eyelid carcinomas. Initial investigations undertaken at simulation of the phantom gave rise to the selection of the lumencath applicator for HDR brachytherapy over other treatment options, based around the flexibility and reproducibility of the catheter and its ability to be shaped easily in conjunction with the use of thermoplastic material. The methods described are not limited to the vendor-specific equipment mentioned and can be adapted to suit other vendors equipment.

Dose was calculated by the brachytherapy treatment planning system, using a standard algorithm based on the TG 43 formalism. The TG 43 formalism assumes everything is water and hence does not include density corrections for the treatment planning. It was therefore necessary to investigate the effects of density heterogeneities (including bone and missing tissue) on the dose derived to the head phantom.

Dosimetry evaluation was completed by using radiochromic film. Results from the radiochromic film measurements gave rise to the selection of the level of thermoplastic bolus used to bring the treatment area and a treatment dose to the closest comparison possible from the prescription and planning data. Film measurements also showed the effect that bone played in the treatment delivery due to its proximity to the catheter in relation to the target volume.

The eye lens dose was also measured both with film and OSLD point measurements. This led to the recommendation that an eye shield should be used during treatment to help reduce the dose to the eye lens and it is also recommended that the eye be rotated superiorly (the patient should be instructed to ‘look up’) to further improve the reduction of the dose to the eye lens. This will lead to dose reduction below the threshold for major side effects to vision from radiation dose to the lens.

In vivo dose measurements are recommended for treatment dose verification (van Dam and Marinello, 1994) however in vivo dosimetry for HDR brachytherapy treatments is notoriously challenging. When performing or investigating in vivo techniques for HDR brachytherapy researchers have reported uncertainties of 3 – 5% for scintillators, up to 10% for film and diamond dosimeters and up to 15% for diodes, with some TLD studies reporting dose variations of up to 60 – 70%

The steep dose fall off from the iridium source was found to be similarly problematic for the OSLD measurements in this study. OSLD measurements were found to perform better when placed a slight distance away from the catheter whereas film can be used in direct contact with the catheter. OSLD measurements can be beneficial when there is a layer of thermoplastic between the catheter and the OSLD chip, however film measurements showed that placing the OSLD between the thermoplastic and the patients skin may have an unacceptable effect on the skin dose, due to scattering effects from the OSLDs.

Despite some disadvantages, it is recommended that OSLDs be used for in vivo measurements to the eye lens, as with practice the uncertainties are reduced, and they provide quick turnaround of dose, so that there is time to alter the treatment plan if necessary. Film requires a lot more manual handling, preparation and individual calibration which can be time prohibitive in a clinical situation, where OSLDs can be batch calibrated and require substantially less time.

The major limitation of this study is the use of the AAPM's TG 43 formalism to calculate the treatment dose, which then required the inaccuracies of the dose calculation to be quantified or mitigated. There has been an updated AAPM report, TG 186 (Beaulieu et al., 2012), that includes algorithms that account for

density variations however these are not widely available due to the potential need to alter prescriptions and report results in combination with TG 43 results.

There was a limitation of bone phantom material available and hence skull was used as a surrogate for orbit bone. The effects of bone may have been over estimated due to the increased thickness of the skull bone compared to the orbit bone.

While several test plans were created, for film calibration and to investigate specific effects (such as density heterogeneity), only one test treatment plan was developed for measurement using the HDR source and a fully constructed treatment mould. This decision was made because it was believed that due to the physical similarity of treatable lower eyelid carcinomas most of the clinical plans would be geometrically similar to the one used. However, it is advised that care is taken when applying the conclusions devised in this study to treatment geometries and schemes that vary greatly from the one described.

This treatment has also not been fully tested on humans so the implications of pressing the thermoplastic mould on top of the cancer are unclear. In particular, it is not known whether this would cause a large amount of discomfort and inability to proceed with this treatment for the patient clinically.

It is recommended that, after confirmation of patient comfort, this new treatment method can be used for lower eyelid carcinomas and the surface mould should be created with thermoplastic sheets and a lumencath catheter. A clinical protocol and specific instructions on preparing, simulating, planning and delivering these treatments are provided in Appendix A and Appendix B. It is also recommended that in vivo dosimetry be performed, especially including OSLD measurements on the eyelids, especially during the first fraction to ensure optimal dose coverage and eye lens sparing. Care should also be taken to ensure that the day to day positioning is kept to a minimum to avoid dosimetric inaccuracies.

7. Conclusion

This thesis has proposed a unique and viable method to treat basal and squamous cell carcinomas of the lower eyelid using superficial HDR brachytherapy by using a catheter and a custom made surface mould.

In order to achieve the advantages this treatment technique of superficial brachytherapy presented over other treatment modalities for basal cell and squamous cell carcinomas of the lower eyelid it is recommended that a single blue Lumencath be used for the treatment and that a suitable thermoplastic mould is created on a patient with no more than 3 mm between the catheter and the surface of the skin, to ensure adequate dosimetric coverage, as well as at least 6 mm of backscatter material on top of the catheter. It should be ensured that the catheter is firmly placed within this mould and that it does not move during treatment and that its location on the skin can be replicated. The treatment plan should follow a single line catheter reconstruction using internal x-ray markers from the CT scan to create the catheter and the dwell positions for the prescription. A lead eye shield has been shown to significantly reduce the dose to the eye lens and further improvements to this can be achieved by educating and ensuring the patient is looking superiorly for the treatment.

It is highly recommended that an ophthalmic review is undertaken pre and post treatment and in vivo dosimetry should be performed at a minimum for the first fraction of the treatment. This is to ensure the correct placement of the mould as well as to monitor the lens dose. Care should be taken to ensure that appropriate correction factors for the dosimeter have been applied if they have been calibrated in a megavoltage photon beam.

Further work that could be undertaken as a result of this treatment method could include the inclusion of a 3D printed bolus mould to replace the use of thermoplastic sheet as well as the use of this method to treat other anatomical regions that are not uniform in shape, such as the ear and the nose. There could

also be investigations of other methods to create the catheter such as overlaying the thermoplastic over a standard or external beam megavoltage face mask. Further dosimetric work could be carried out with different encasing types over the lead eye shield, for example red dental wax. Additional research could be undertaken to assess the feasibility of combining this novel HDR brachytherapy technique with other treatment modalities, such as surgery.

LOWER EYELID BRACHYTHERAPY Clinical Protocol

Contents

1. Introduction and Background

Cancers of the eyelid account for 59% of all skin cancers, and are responsible for 11% of mortalities arising from skin malignancies. Eyelid cancer can be a therapeutic challenge due to the cosmetic and functional implications of the orbital anatomical region, including preserving the function of the eyelids, and the objectives of therapy such as tumour control as well as functional and cosmetic outcomes.

About 90% of eyelid malignancies are Basal cell carcinoma (BCC), and squamous cell carcinomas make up the remaining majority. BCC are locally invasive; however, they do not metastasise. SCC is a more invasive tumour, and migrates to distant sites via the lymphatic system.

Early treatment techniques (from the 1950s) included different treatment modalities such as superficial x-rays, orthovoltage x-rays, electron beam irradiation, High Dose Rate (HDR) brachytherapy and megavoltage photons.

In 2007 he first published paper on HDR brachytherapy for lower eyelid treatments appeared. This detailed a method for interstitial brachytherapy following surgical excision of the tumour. It was noted that the larger size of the catheter for a HDR source was an issue for treatment. The report noted good outcomes for the patients, both cosmetically and in terms of tumour control.

Electronic Brachytherapy was approved in America in 2009. Due to the lower amount of shielding required and the ability to treat patients

external to a radiotherapy department, such as in a dermatology office, there has been a large increase in this type of treatment for lower eyelid cancers.

Apart from in conjunction with surgery, as yet there is no literature on HDR superficial brachytherapy. A method of treating these BCC and SCC with superficial catheters, originally used for bile duct or bronchial treatments has been created utilising a thermoplastic mould placed over the treatment region to provide optimum coverage and minimal air gaps. This has been verified using in-vivo dosimetry and provides an alternate treatment for these lesions without the cosmetic and invasive need for surgical intervention.

2. Drawbacks of Lower Eyelid Brachytherapy

- No long term studies on outcome available
- Unique treatment method
- Pressure around the treatment site during creation of the mould might cause discomfort

3. Patient Selection

Inclusion criteria

- Basal cell or squamous cell carcinoma of the lower eyelid
- Clear margins, no underlying involvement
- Ability to follow verbal guidance
- Ability to move eye superior and hold for fraction duration
- Lesion size able to be treated effectively with one catheter

- Tumour unable to be effectively or fully surgically resected
- Patient not fit for surgery
- Patients with a recurrence of the lesion after surgical excision

Exclusion criteria

- Previous radiation therapy to the region – RO discretion
- External beam failure –RO discretion

4. Radiotherapy Planning – CT Session

- Patient is informed of the process of making the eye mould with catheter
- Mould is constructed using established guidelines in the work instruction document in conjunction with the RO outline
- CT scan of the relevant region on head is taken using established CT protocol
- mould is removed with catheter for storage until treatment commences

5. Nurses Talk

Nurses will do the patient information talk using the patient education template in MOSAIQ.

This will ensure consistency in the information given to the patient.

6. Contouring

- Undertaken by the RT, using existing protocols
- outlining the catheter, orbit, lens underling cartilage and other structures as requested by the RO

7. Dosimetry

- Standard planning for bile duct/bronchus

- Plan as normal, on scan without marker wires, ensuring even dose coverage
- RO to review plan and approve – dose constraints to target and organs at risk (lens, underlying cartilage, skin max/min dose)
- Common prescription and fractionation for skin is 3 – 4 Gy three times a week or 1.8 Gy five days a week, at the ROs discretion.
- Organ at risk tolerances – as per current eviQ guidelines

8. Treatment Delivery

- Treatment delivery performed on the Elekta HDR unit with Ir-192 source
- Setup using CT setup notes including tracings to ensure reproducibility
- Shielding as required to be used around the eye

9. Treatment Verification

- Daily matching to simulation diagram
- Check treatment unit source strength and dwell times for each position match planned times

10. Outcome Measurement

Once the patient commences treatment, follow-ups will conform to existing HDR protocols, and RO will measure outcomes of treatment

11. Follow-up schedule

- Patient can continue followed up telephonically every six months and called for a review appointment if symptoms/complications are suspected
- Ophthalmologic review pre and post treatment conclusion for the first five patients

12. Appendix

Workflow

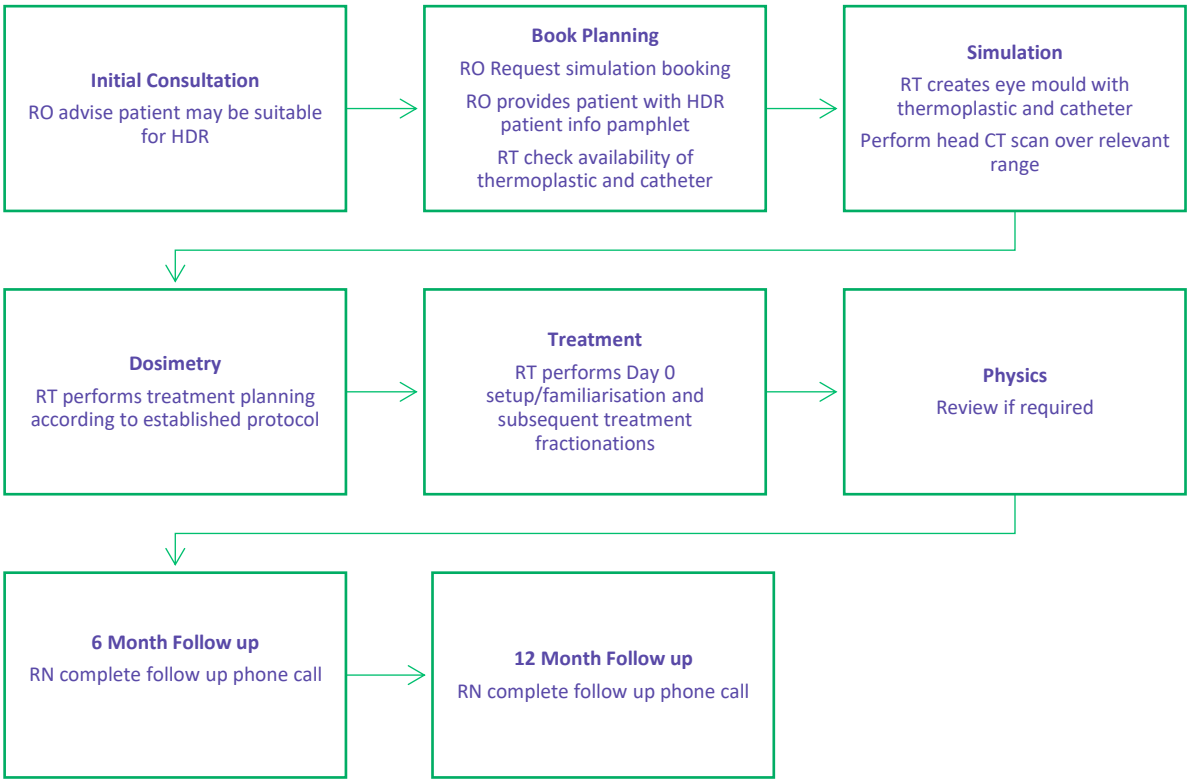

Keywords

Eyelid
Brachytherapy

Work Instruction HDR Lower Eyelid Brachytherapy

Contents

1. Purpose

This document should be used as a memory aid for qualified individuals and/or as a guide for trainees undertaking supervised training in HDR.

2. Scope

This work instruction is specifically applicable to the safe and appropriate use of HDR treatment by those who are both licensed to deliver HDR treatment and those suitably trained in such procedures under the supervision of licensed users of brachytherapy treatment delivery.

This protocol must be read in conjunction with the relevant Radiation Safety and Protection Plans (RSPPs) for brachytherapy and reference to procedures of the following documents is essential as part of completing this work procedure:

- HDR Document Preparation
- HDR Dosimetry Check
- HDR Pre-Treatment Check
- HDR Treatment Procedure

3. Legislative compliance

3.1 National Safety and Quality Standards

Standard 1.12: Ensuring that systems are in place for ongoing safety and quality education and training.

3.2 Radiation Safety Act

This work instruction conforms to the requirements of the Genesis Cancer Care Queensland (GCCQ) Radiation Safety & Protection Plan, 2015

4. Procedure

Lower eyelid carcinomas are treated with HDR radiation to obtain a curative intent without external beam radiation. They are used as a primary option in lieu of surgery, alternatively the treatment can be carried out after surgical resection.

4.1 Equipment Preparation

The Bronc/Oesophagus kit will be required (Figure WI 1). The Lumencath Treatment Catheter are purchased as sterile units. The Bronchial/Oesophageal Applicator and the X-ray marker wire do not require sterilisation. Thermoplastic pieces, either the small cylindrical pellets or small rectangular pieces will be required to form the mould. The

marker wire should be retained in the catheter to ensure effective rigidity during the creation of the mould to maintain catheter shape

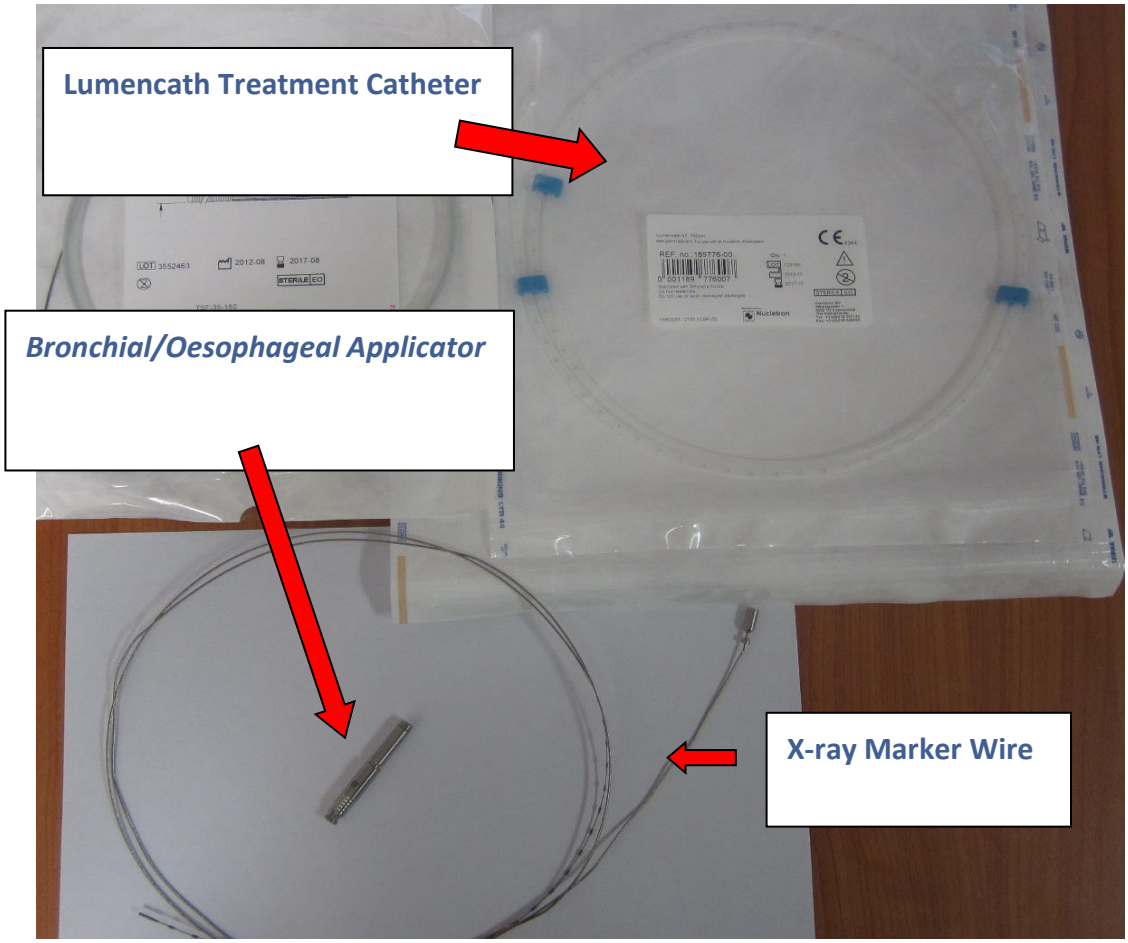

Figure WI 1 Generic Bronc/Oesophagus kit from Elekta

4.2 Mould Creation

The mould to sit on the lower eyelid is constructed from thermoplastic. The base layer is shaped according to the doctors' outline on the skin. (Figure WI 2)

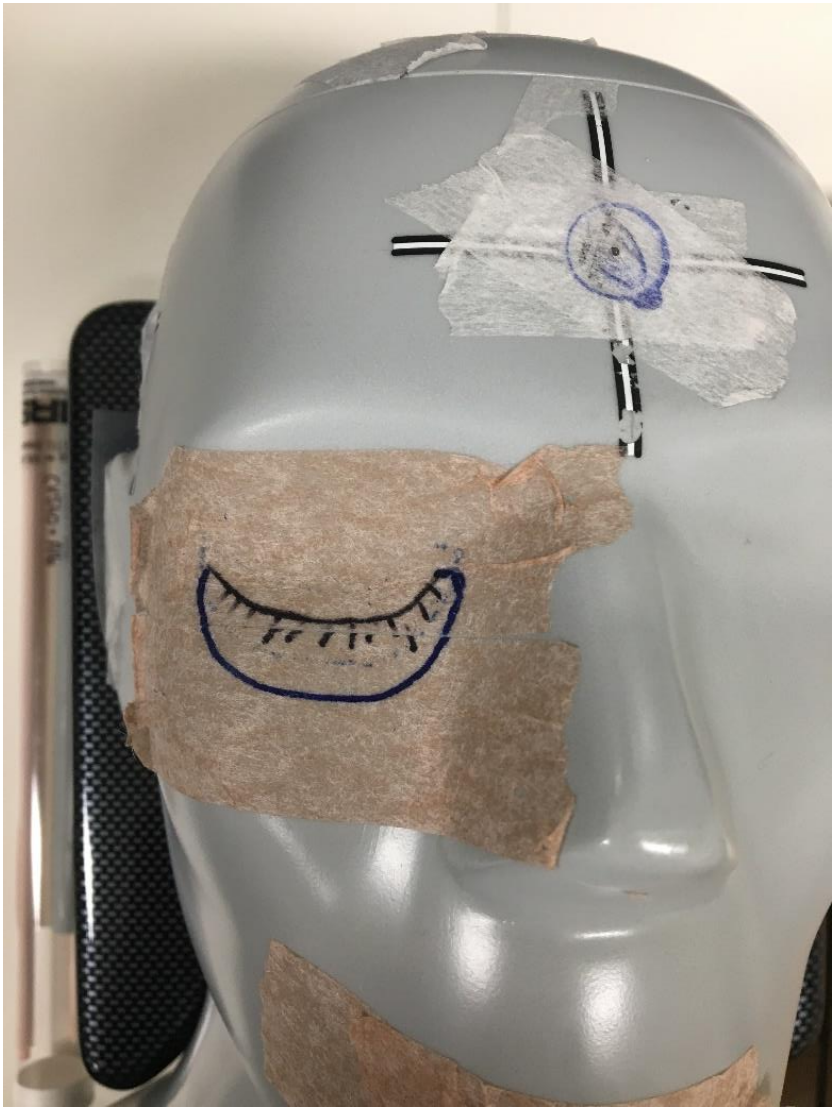

Figure WI 2 Outline on phantom to show thermoplastic location

Submerge a small sheet of thermoplastic in a water bath to soften and cut with scissors to the shape marked on the skin. The catheter is placed on top whilst warm, ensuring that the clinical target volume for the carcinoma

is covered – this being the palpable/visible tumour with a 3 -5 mm safety margin, and is aligned to the centre of the marked volume. Ensure the catheter maintains at least 3 mm separation between the posterior portion of the catheter and the thermoplastic to the skin.

At least two pieces of softened thermoplastic are then placed on top to help hold in place (Figure WI 3). Alternatively, the mould can be created with thermoplastic pellets, ensuring at least 5 mm plastic is present on top of the catheter and at least 3 mm between the catheter and skin. The catheter remains in this mould for the duration of the treatment and is not removed from the mould between fractions. Mark the catheter with the edges of the mould to ensure the catheter maintains its position within the mould itself.

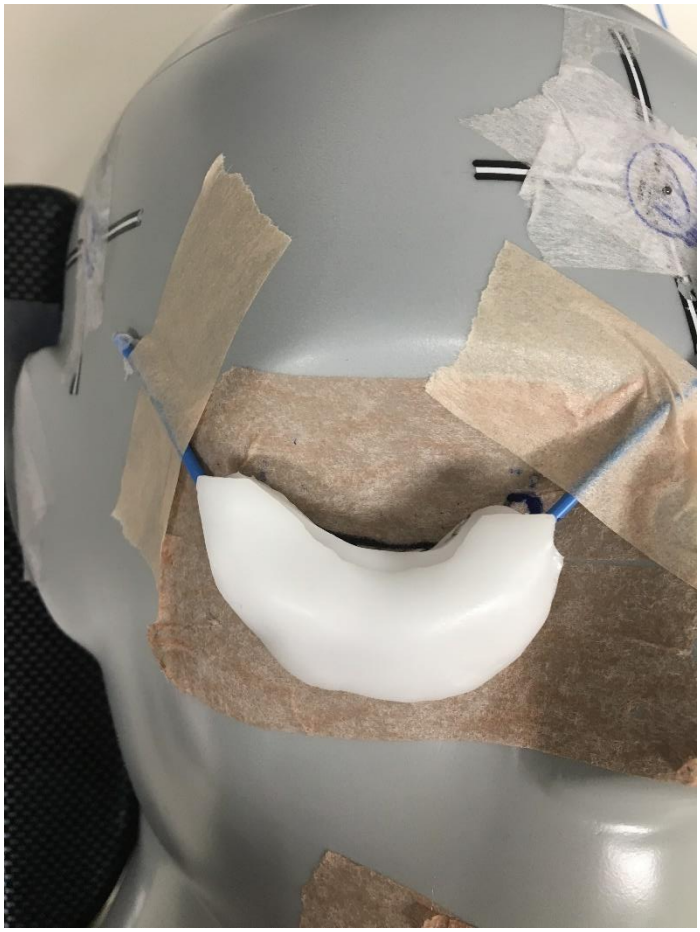

Figure WI 3 Completed thermoplastic mould

4.3 Simulation

The patient will require a CT scan for planning purposes. This is performed on a CCQ CT scanner. The patient is scanned in the supine head protocol simulation position. The outline of the eye mould can be surrounded with marker wire and the x-ray marker wire is inside the catheter for scanning. The scan should include the region to be treated plus an appropriate upper and lower margin.

Prior to export the CT data should be checked to confirm that there is a minimal/absent air gap between the skin and the surface mould. The scan should then be exported from the CT.

A tracing of the skin markings should be taken and photographs of the area.

4.4 Dosimetry

4.4.1 Patient Creation

Start the import module in Oncentra 

Import from desktop by changing the source directory to \\Wesleydc\Dicom

Select the patient from the list then the CT scan from the drop-down menu

A new patient will need to be created (Figure WI 4). Select **Create New Patient**. Add info as required. Select **OK.** Import the CT slices into the patient

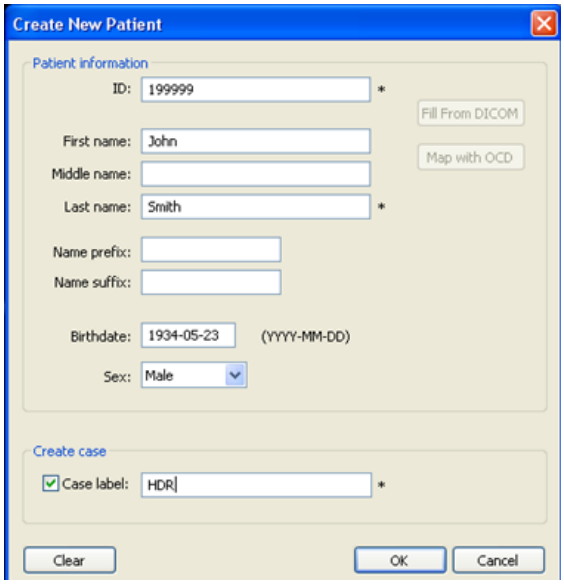

Figure WI 4 New Patient window

The following window (Figure WI 5) showing the Case for the plan will appear. Leave this window open.

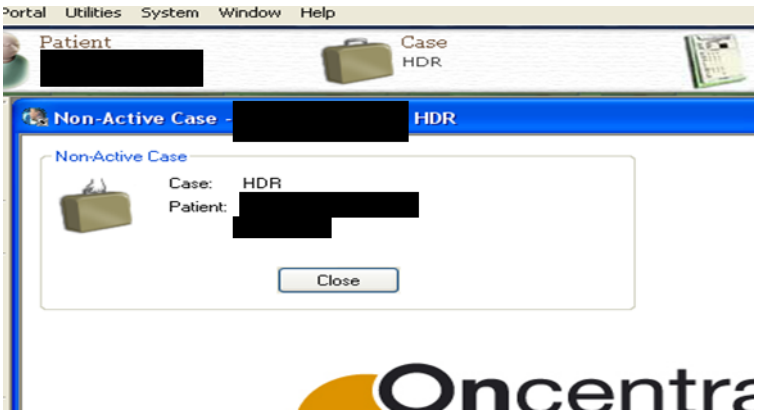

Figure WI 5 New Case Window

The treatment area can be obtained from the CT scan.

4.4.2 Reconstruction

Digitise from the tip end with a minimum source step size of 2.5 mm, a little more than the treatment length in both the sup and inf directions (NB. The most distal treatable point is the gap between the double markers at the most distal end of the catheter) The end of the catheter is at 1500 mm (no dead space) but as the check cable travels further than the 1500 mm. If the first digitised point is at the tip of the catheter, then an offset of -5 mm can be applied (Figure WI 6)

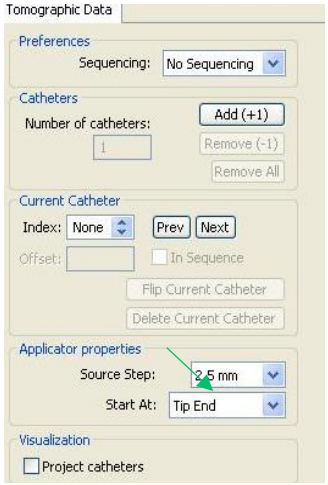

Figure WI 6 Catheter reconstruction and activated positions

Highlight the treatment length; be sure to not activate any extra-digitised length

Select all catheters and activate all.

4.4.3 Points

Points need to be generated by selecting the add points icon (Figure WI 7)

Figure WI 7 Location of 'add points' icon

Select 'Catheter' points from the menu and add the prescribed distance to the minimal distance dialogue box.

The following window will open (Figure WI 8)

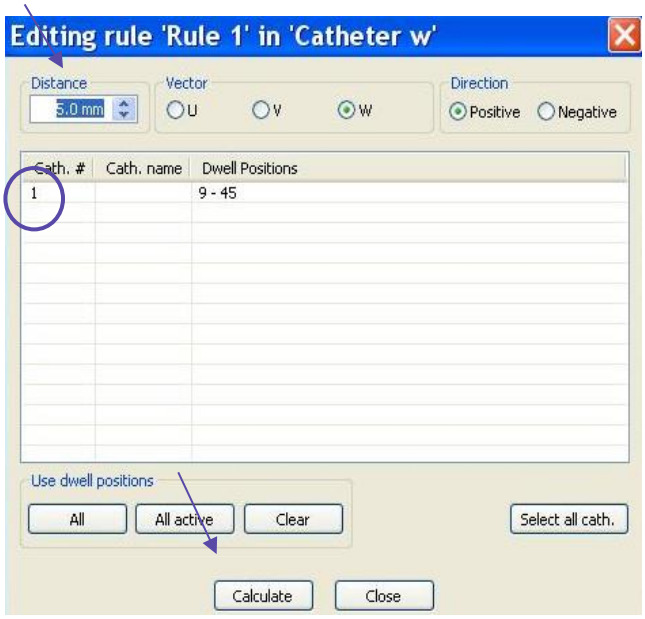

Figure WI 8 Catheter Distance window

Enter the prescribed distance.

The vector coordinate is relative to the catheter. It places the points around the catheter at the prescribed distance and can be changed if the placement is not optimal.

Select the catheter and click all active. The dwell positions should appear. Calculate.

The points should be evenly spread along the catheter as demonstrated below (Figure WI 9). To view from the 3D perspective, click the ECS view button and drag the 3D image into the main window. The points should not be 'bunched' in the curve of the catheter.

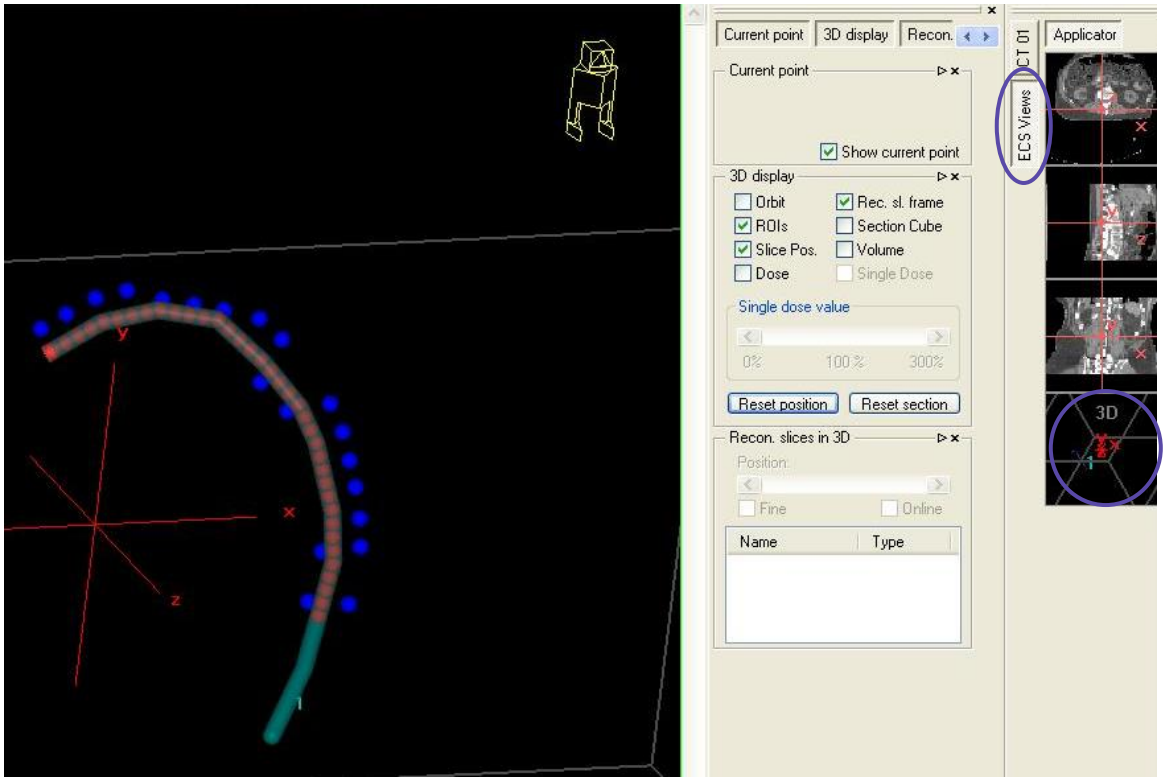

Figure WI 9 Screenshot of un-bunched, well placed dwell positions

4.4.4 Normalisation

Normalise to the catheter points (Figure WI 10)

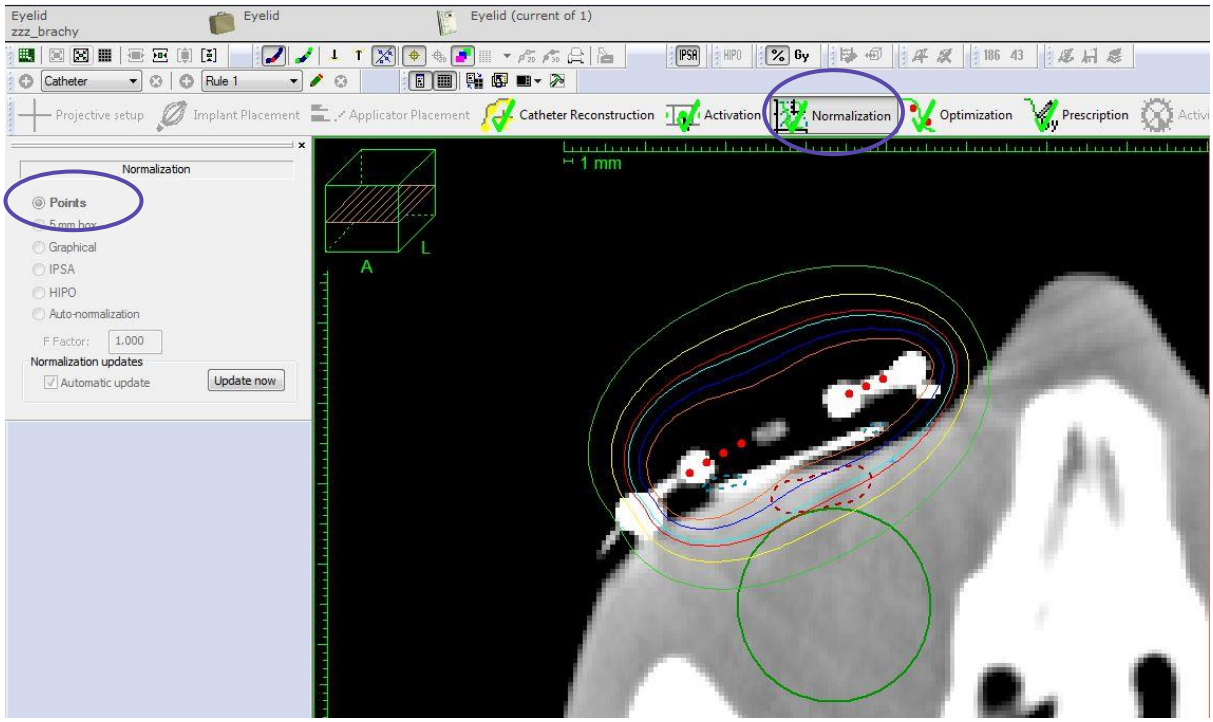

Figure WI 10 Normalisation to catheter points location

4.4.5 Optimisation

Optimise to points (Figure WI 11)

The dwell points should then change to larger dwells on the ends of the treatment length.

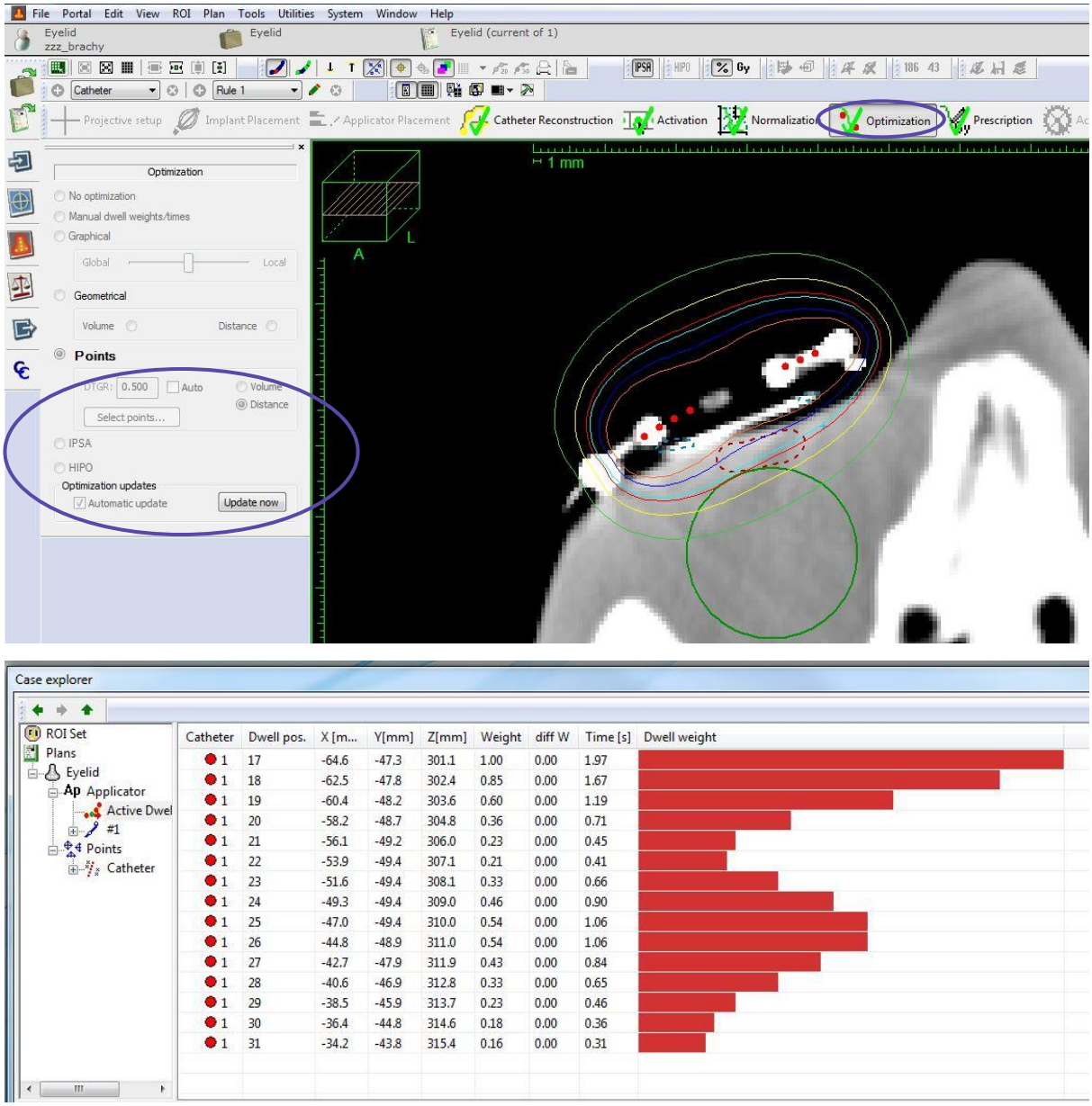

Figure WI 11 Optimisation of points

Optimise Geometrical distance if required to lower dose to any OAR's.

4.4.6 Dose and Fractionation

The current fractionation is under review.

To view the 3D dose cloud, from the 'Plan' drop down menu select 'Calculate 3D Dose'. In the 'Properties' tab select the 'Dose' tick box (Figure WI 12)

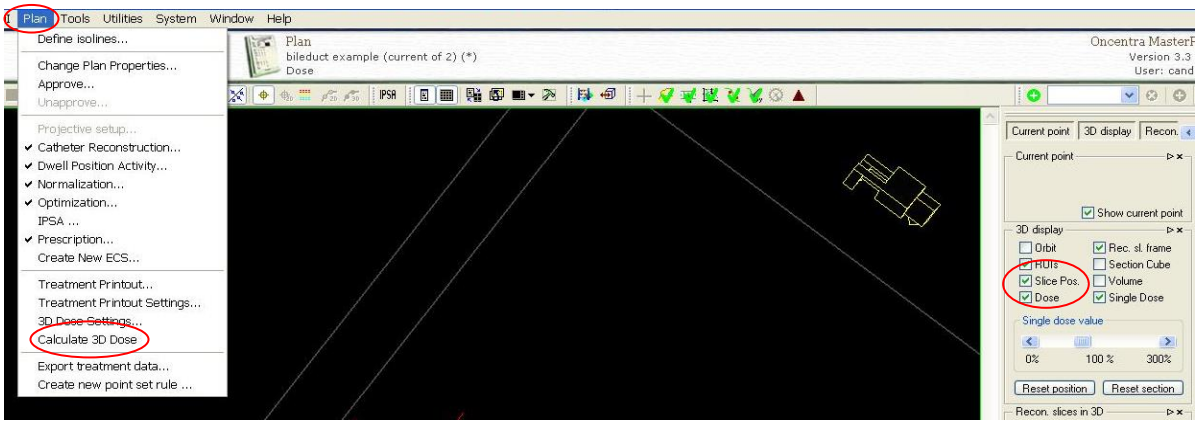

Figure WI 12 3D dose cloud settings

The 3D dose distribution should look as displayed below (Figure WI 13) with the 100% dose cloud touching the points in a 'sausage like' configuration.

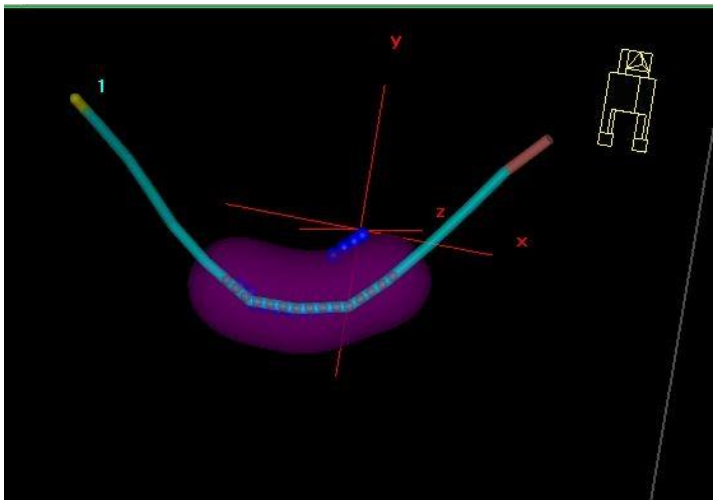

Figure WI 13 3D dose cloud

4.4.7 Dosimetry Checking

Refer to Dosimetry Checking Document

5. Pre-Treatment Checks

Before delivery of the treatment there are several steps that have to be performed. These steps are universal for all brachytherapy treatments regardless of disease site and are essential for treatment.

Import the plan into the TCS. This is done following plan approval and only needs to be performed once.

Perform plan importing and pre-treatment checks as per the Brachytherapy Pre-treatment Check document.

6. Treatment Delivery

Ensure the x-ray marker wire is removed from the catheter before inserting into number '1' on the indexer ring. Retain the x-ray marker wire to re-insert into the catheter to ensure its integrity. The catheter is to be stored by gently winding it and storing with the eye mould still attached for future fractionations.

Treatment delivery should only be delivered by a suitably licensed Radiation Therapist or Physicist according to the RSPP. Please refer to this document for emergency procedures.

The separate Treatment Procedure document should also be referred to.

References

ALAM, M., NANDA, S., MITTAL, B. B., KIM, N. A. & YOO, S. 2011. The use of brachytherapy in the treatment of nonmelanoma skin cancer: a review. *Journal of the American Academy of Dermatology,* 65**,** 377-388.

ALAND, T., KAIRN, T. & KENNY, J. 2011. Evaluation of a Gafchromic EBT2 film dosimetry system for radiotherapy quality assurance. *Australasian physical & engineering sciences in medicine,* 34**,** 251-260.

ALECU, R. & ALECU, M. 1999. In-vivo rectal dose measurements with diodes to avoid misadministrations during intracavitary high dose rate brachytherapy for carcinoma of the cervix. *Med Phys,* 26**,** 768-70.

ANAGNOSTOPOULOS, G., BALTAS, D., PANTELIS, E., PAPAGIANNIS, P. & SAKELLIOU, L. 2004. The effect of patient inhomogeneities in oesophageal 192Ir HDR brachytherapy: a Monte Carlo and analytical dosimetry study. *Physics in Medicine & Biology,* 49**,** 2675.

ARNOTT, S., LAW, J., ASH, D., FLYNN, A., PAINE, C., DURRANT, K., BARBER, C. & DIXON-BROWN, A. 1985. Problems associated with iridium-192 wire implants. *Clinical radiology,* 36**,** 283-285.

ATTIX, F. H. 2008. *Introduction to radiological physics and radiation dosimetry*, John Wiley & Sons.

AZAD, S. & CHOUDHARY, V. 2011. Treatment results of high dose rate interstitial brachytherapy in carcinoma of eye lid. *Journal of Cancer Research and Therapeutics,* 7**,** 157-161.

BALTAS, D., GERAMANI, K., IOANNIDIS, G. T., HIERHOLZ, K., ROGGE, B., KOLOTAS, C., MÜLLER-SIEVERS, K., MILICKOVIC, N., KOBER, B. & ZAMBOGLOU, N. 1999. Comparison of calibration procedures for 192Ir high-dose-rate brachytherapy sources. *International Journal of Radiation Oncology* Biology* Physics,* 43**,** 653-661.

BEAULIEU, L., CARLSSON TEDGREN, Å., CARRIER, J. F., DAVIS, S. D., MOURTADA, F., RIVARD, M. J., THOMSON, R. M., VERHAEGEN, F., WAREING, T. A. & WILLIAMSON, J. F. 2012. Report of the Task Group 186 on model-based dose calculation methods in brachytherapy beyond the TG-43 formalism: current status and recommendations for clinical implementation. *Medical physics,* 39**,** 6208-6236.

BELL, S. 1999. A beginner's guide to uncertainty of measurement. *Measurement good practice guide,* 11**,** 1.

BENSALEH, S., BEZAK, E. & BORG, M. 2009. Review of MammoSite brachytherapy: advantages, disadvantages and clinical outcomes. *Acta Oncologica,* 48**,** 487-494.

BUTSON, M. J., CHEUNG, T. & YU, P. K. 2008. Measuring energy response for RTQA radiochromic film to improve quality assurance procedures. *Australasian Physics & Engineering Sciences in Medicine,* 31**,** 203-206.

CROWSON, A. N. 2006. Basal cell carcinoma: biology, morphology and clinical implications. *Modern pathology,* 19**,** S127.

DALY, N. J., DE LAFONTAN, B. & COMBES, P. F. 1984. Results of the treatment of 165 lid carcinomas by iridium wire implant. *International Journal of Radiation Oncology• Biology• Physics,* 10**,** 455-459.

DELISHAJ, D., LALISCIA, C., MANFREDI, B., URSINO, S., PASQUALETTI, F., LOMBARDO, E., PERRONE, F., MORGANTI, R., PAIAR, F. & FABRINI, M. G. 2015. Non-melanoma skin cancer treated with high-dose-rate brachytherapy and Valencia applicator in elderly patients: a retrospective case series. *Journal of contemporary brachytherapy,* 7**,** 437.

DEVIC, S. 2011. Radiochromic film dosimetry: past, present, and future. *Physica medica,* 27**,** 122-134.

DEVIC, S., SEUNTJENS, J., SHAM, E., PODGORSAK, E. B., SCHMIDTLEIN, C. R., KIROV, A. S. & SOARES, C. G. 2005. Precise radiochromic film dosimetry using a flat-bed document scanner. *Med Phys,* 32**,** 2245-53.

DUNN, L., LYE, J., KENNY, J., LEHMANN, J., WILLIAMS, I. & KRON, T. 2013. Commissioning of optically stimulated luminescence dosimeters for use in radiotherapy. *Radiation Measurements,* 51**,** 31-39.

FIRNHABER, J. M. 2012. Diagnosis and treatment of Basal cell and squamous cell carcinoma. *Am Fam Physician,* 86**,** 161-8.

FRAKULLI, R., GALUPPI, A., CAMMELLI, S., MACCHIA, G., CIMA, S., GAMBACORTA, M. A., CAFARO, I., TAGLIAFERRI, L., PERRUCCI, E., BUWENGE, M., FREZZA, G., VALENTINI, V. & MORGANTI, A. G. 2015. Brachytherapy in non melanoma skin cancer of eyelid: a systematic review. *Journal of Contemporary Brachytherapy,* 7**,** 497-502.

FREDERICK L, G., PAGE, D. L., FLEMING, I. D., FRITZ, A. G., BALCH, C. M., HALLER, D. G. & MORROW, M. 2013. *AJCC Cancer Staging Manual*, Springer New York.

GUINOT, J. L., REMBIELAK, A., PEREZ-CALATAYUD, J., RODRIGUEZ-VILLALBA, S., SKOWRONEK, J., TAGLIAFERRI, L., GUIX, B., GONZALEZ-PEREZ, V., VALENTINI, V. & KOVACS, G. 2018. GEC-ESTRO ACROP recommendations in skin brachytherapy. *Radiother Oncol,* 126**,** 377-385.

GUIX, B., FINESTRES, F., TELLO, J.-I., PALMA, C., MARTINEZ, A., GUIX, J.-R. & GUIX, R. 2000a. Treatment of skin carcinomas of the face by high-dose-rate brachytherapy and custom-made surface molds. *International Journal of Radiation Oncology*Biology*Physics,* 47**,** 95-102.

GUIX, B., FINESTRES, F., TELLO, J., PALMA, C., MARTINEZ, A., GUIX, J. & GUIX, R. 2000b. Treatment of Skin Carcinomas of the Face by High Dose Rate Brachytherapy and Custom Made Surface Molds. *Int J Radiat Oncol Biol Phys,* 47.

HANSEN, E. & ROACH, M. 2006. *Handbook of Evidence-based Radiation Oncology*, Springer New York.

HAUGHEY, A., COALTER, G. & MUGABE, K. 2011. Evaluation of linear array MOSFET detectors for in vivo dosimetry to measure rectal dose in HDR brachytherapy. *Australas Phys Eng Sci Med,* 34**,** 361-6.

IAEA 2013. *Development of Procedures for In Vivo Dosimetry in Radiotherapy,* Vienna, INTERNATIONAL ATOMIC ENERGY AGENCY.

ISLAM, M. A., AKRAMUZZAMAN, M. M. & ZAKARIA, G. A. 2012. Dosimetric comparison between the microSelectron HDR (192)Ir v2 source and the BEBIG (60)Co source for HDR brachytherapy using the EGSnrc Monte Carlo transport code. *Journal of medical physics,* 37**,** 219-225.

JURSINIC, P. A. 2007. Characterization of optically stimulated luminescent dosimeters, OSLDs, for clinical dosimetric measurements. *Medical physics,* 34**,** 4594-4604.

KAPREALIAN, T., MISHRA, K. K., WANG-CHESEBRO, A. & QUIVEY, J. M. 2010. Malignant and Benign Diseases of the Eye and Orbit. *In:* HANSEN, E. K. & ROACH, M. (eds.) *Handbook of Evidence-Based Radiation Oncology.* New York, NY: Springer New York.

KASSAS, B., MOURTADA, F., HORTON, J. L., LANE, R. G., BUCHHOLZ, T. A. & STROM, E. A. 2006. Dose modification factors for 192Ir high-dose-rate irradiation using Monte Carlo simulations. *Journal of applied clinical medical physics,* 7**,** 28-34.

KIROV, A. S., WILLIAMSON, J. F., MEIGOONI, A. & ZHU, Y. 1995. TLD, diode and Monte Carlo dosimetry of an 192Ir source for high dose-rate brachytherapy. *Physics in Medicine & Biology,* 40**,** 2015.

KOTWALL, C., SAKO, K., RAZACK, M. S., RAO, U., BAKAMJIAN, V. & SHEDD, D. P. 1987. Metastatic patterns in squamous cell cancer of the head and neck. *The American Journal of Surgery,* 154**,** 439-442.

KRENGLI, M., MASINI, L., COMOLI, A., NEGRI, E., DEANTONIO, L., FILOMENO, A. & GAMBARO, G. 2014. Interstitial brachytherapy for eyelid carcinoma. *Strahlentherapie und Onkologie,* 190**,** 245.

KRON, T. 1994. Thermoluminescence dosimetry and its applications in medicine--Part 1: Physics, materials and equipment. *Australasian physical & engineering sciences in medicine,* 17**,** 175-199.

KUTCHER, G., COIA, L. & GILLIN, M. 1994. Comprehensive QA for radiation oncology. Report of Task Group No. 40 of the Radiation Therapy Committee of the American Association of Physicists in Medicine. AAPM Report.

LAMBERT, J., NAKANO, T., LAW, S., ELSEY, J., MCKENZIE, D. R. & SUCHOWERSKA, N. 2007. In vivo dosimeters for HDR brachytherapy: a comparison of a diamond detector, MOSFET, TLD, and scintillation detector. *Med Phys,* 34**,** 1759-65.

MANGHANI, J. & KHAN, K. 2016. A study of role of brachytherapy IR192 in treatment of eyelid tumors. *International Journal of Medical Research and Review,* 4.

MANIKANDAN, A., BIPLAB, S., DAVID, P. A., HOLLA, R., VIVEK, T. & SUJATHA, N. 2011. Relative dosimetrical verification in high dose rate brachytherapy using two-dimensional detector array IMatriXX. *Journal of Medical Physics/Association of Medical Physicists of India,* 36**,** 171.

MARTINEZ-MONGE, R. & GOMEZ-ITURRIAGA, A. 2007. High-dose-rate brachytherapy in lower eyelid cancer. *Brachytherapy,* 6**,** 227-9.

MILLE, M. M., XU, X. G. & RIVARD, M. J. 2010. Comparison of organ doses for patients undergoing balloon brachytherapy of the breast with HDR or electronic sources using Monte Carlo simulations in a heterogeneous human phantom a. *Medical physics,* 37**,** 662-671.

NATH, R., ANDERSON, L. L., LUXTON, G., WEAVER, K. A., WILLIAMSON, J. F. & MEIGOONI, A. S. 1995. Dosimetry of interstitial brachytherapy sources:

Recommendations of the AAPM Radiation Therapy Committee Task Group No. 43. *Medical Physics,* 22**,** 209-234.

NIU, H., HSI, W. C., CHU, J. C. H., KIRK, M. C. & KOUWENHOVEN, E. 2004. Dosimetric characteristics of the Leipzig surface applicators used in the high dose rate brachy radiotherapy. *Med Phys,* 31.

OUHIB, Z., KASPER, M., CAATAYUD, J. P., RODRIGUEZ, S., BHATNAGAR, A., PAIS, S. & STRASSWIMRNER, J. 2015. Aspects of dosimetry and clinical practice of skin brachytherapy: The American Brachytherapy Society working group report. *Brachytherapy,* 14**,** 840-858.

OZGEDIZ, D., SMITH, E., ZHENG, J., OTERO, J., TABATABAI, Z. L. & CORVERA, C. U. 2008. Basal cell carcinoma does metastasize. *Dermatology Online Journal,* 14.

PAI, S., REINSTEIN, L. E., GLUCKMAN, G., XU, Z. & WEISS, T. 1998. The use of improved radiochromic film for in vivo quality assurance of high dose rate brachytherapy. *Med Phys,* 25**,** 1217-21.

PANTELIS, E., PAPAGIANNIS, P., KARAISKOS, P., ANGELOPOULOS, A., ANAGNOSTOPOULOS, G., BALTAS, D., ZAMBOGLOU, N. & SAKELLIOU, L. 2005. The effect of finite patient dimensions and tissue inhomogeneities on dosimetry planning of 192Ir HDR breast brachytherapy: a Monte Carlo dose verification study. *International Journal of Radiation Oncology* Biology* Physics,* 61**,** 1596-1602.

PAULSEN, F. 2012. *The Human Nasolacrimal Ducts*, Springer Berlin Heidelberg.

PEET, S. C., WILKS, R., KAIRN, T., TRAPP, J. V. & CROWE, S. B. 2016. Calibrating radiochromic film in beams of uncertain quality. *Medical physics,* 43**,** 5647-5652.

PETROKOKKINOS, L., ZOURARI, K., PANTELIS, E., MOUTSATSOS, A., KARAISKOS, P., SAKELLIOU, L., SEIMENIS, I., GEORGIOU, E. & PAPAGIANNIS, P. 2011. Dosimetric accuracy of a deterministic radiation transport based 192Ir brachytherapy treatment planning system. Part II: Monte Carlo and experimental verification of a multiple source dwell position plan employing a shielded applicator. *Med Phys,* 38**,** 1981-92.

POON, E., LE, Y., WILLIAMSON, J. F. & VERHAEGEN, F. BrachyGUI: an adjunct to an accelerated Monte Carlo photon transport code for patient-specific brachytherapy dose calculations and analysis. Journal of Physics: Conference Series, 2008. IOP Publishing, 012018.

QI, Z. Y., DENG, X. W., HUANG, S. M., LU, J., LERCH, M., CUTAJAR, D. & ROSENFELD, A. 2007. Verification of the plan dosimetry for high dose rate brachytherapy using metal–oxide–semiconductor field effect transistor detectors. *Medical physics,* 34**,** 2007-2013.

REIFLER, D. M. & HORNBLASS, A. 1986. Squamous cell carcinoma of the eyelid. *Survey of Ophthalmology,* 30**,** 349-365.

RIVARD, M. J., COURSEY, B. M., DEWERD, L. A., HANSON, W. F., HUQ, M. S., IBBOTT, G. S., MITCH, M. G., NATH, R. & WILLIAMSON, J. F. 2004. Update of AAPM Task Group No. 43 Report: A revised AAPM protocol for brachytherapy dose calculations. *Med Phys,* 31**,** 633-74.

RIVARD, M. J., DAVIS, S. D., DEWERD, L. A., RUSCH, T. W. & AXELROD, S. 2006. Calculated and measured brachytherapy dosimetry parameters in water

for the Xoft Axxent X-Ray Source: An electronic brachytherapy source a. *Medical physics,* 33**,** 4020-4032.

SAFAI, B. & GOOD, R. A. 1977. Basal cell carcinoma with metastasis. Review of literature. *Archives of pathology & laboratory medicine,* 101**,** 327-331.

SARFEHNIA, A., KAWRAKOW, I. & SEUNTJENS, J. 2010. Direct measurement of absorbed dose to water in HDR brachytherapy: Water calorimetry, ionization chamber, Gafchromic film, and TG-43. *Medical physics,* 37**,** 1924-1932.

SEMRAU, S., KUNZ, M., BAGGESEN, K., VOGEL, H., BUCHMANN, W., GROSS, G. & FIETKAU, R. 2008. *Successful treatment of field cancerization of the scalp by surface mould brachytherapy*.

SNELL, R. S. & LEMP, M. A. 2013. *Clinical Anatomy of the Eye*, Wiley.

SOMANCHI, B., STANTON, A., WEBB, M., LONCASTER, J., ALLAN, E. & MUIR, L. 2008. Hand function after high dose rate brachytherapy for squamous cell carcinoma of the skin of the hand. *Clinical oncology,* 20**,** 691-697.

SOYSAL, H. G. & MARKOÇ, F. 2007. Invasive squamous cell carcinoma of the eyelids and periorbital region. *British Journal of Ophthalmology,* 91**,** 325-329.

SPEZI, E., ANGELINI, A., ROMANI, F. & FERRI, A. 2005. Characterization of a 2D ion chamber array for the verification of radiotherapy treatments. *Physics in Medicine & Biology,* 50**,** 3361.

SULLIVAN, D. A., STERN, M. E., TSUBOTA, K., DARTT, D. A., SULLIVAN, R. M. & BROMBERG, B. B. 2003. *Lacrimal Gland, Tear Film, and Dry Eye Syndromes 3: Basic Science and Clinical Relevance*, Springer US.

SYMONDS, R. P., DEEHAN, C., MEREDITH, C. & MILLS, J. A. 2012. *Walter and Miller's Textbook of Radiotherapy: Radiation Physics, Therapy and Oncology*, Elsevier Health Sciences UK.

THERRIAULT-PROULX, F., BRIERE, T. M., MOURTADA, F., AUBIN, S., BEDDAR, S. & BEAULIEU, L. 2011. A phantom study of an in vivo dosimetry system using plastic scintillation detectors for real-time verification of 192Ir HDR brachytherapy. *Med Phys,* 38**,** 2542-51.

TORMO, A., CELADA, F., RODRIGUEZ, S., BOTELLA, R., BALLESTA, A., KASPER, M., OUHIB, Z., SANTOS, M. & PEREZ-CALATAYUD, J. 2014. Non-melanoma skin cancer treated with HDR Valencia applicator: clinical outcomes. *Journal of contemporary brachytherapy,* 6**,** 167.

TOYE, W., DAS, R., KRON, T., FRANICH, R., JOHNSTON, P. & DUCHESNE, G. 2009. An in vivo investigative protocol for HDR prostate brachytherapy using urethral and rectal thermoluminescence dosimetry. *Radiotherapy and Oncology,* 91**,** 243-248.

TURVEY, T. A. & GOLDEN, B. A. 2012. Orbital Anatomy for the Surgeon. *Oral and maxillofacial surgery clinics of North America,* 24**,** 525-536.

VAN DAM, J. & MARINELLO, G. 1994. *Methods for in Vivo Dosimetry in External Radiotherapy*, Garant Publ.

WEINSTOCK, M. A., BOGAARS, H. A., ASHLEY, M., LITLE, V., BILODEAU, E. & KIMMEL, S. 1991. Nonmelanoma skin cancer mortality: a population-based study. *Archives of dermatology,* 127**,** 1194-1197.

XU, X., ZHAO, S., LIU, H., SUN, Z., WANG, J. & ZHANG, W. 2017. An Anatomical Study of Maxillary-Zygomatic Complex Using Three-Dimensional Computerized Tomography-Based Zygomatic Implantation. *BioMed research international,* 2017.

YAHNKE, C. J. 2009. Calibrating the microStar. *Rev.,* 2.

YUKIHARA, E. G. & MCKEEVER, S. W. S. 2011. *Optically Stimulated Luminescence: Fundamentals and Applications*, Wiley.

ZHANG, M., ZHANG, L., YUAN, S. & DAI, G. 2010. A study of experimental measurements of dosimetric parameters in HDR Ir-192 source. *Medical Dosimetry,* 35**,** 250-254.

ZHANG, Z., PARSAI, E. I. & FELDMEIER, J. J. 2007. Three-dimensional quantitative dose reduction analysis in MammoSite balloon by Monte Carlo calculations. *J Appl Clin Med Phys,* 8**,** 2669.

ZILIO, V. O., JONEJA, O. P., POPOWSKI, Y., ROSENFELD, A. & CHAWLA, R. 2006. Absolute depth-dose-rate measurements for an HDR brachytherapy source in water using MOSFET detectors. *Medical physics,* 33**,** 1532-1539.